

## Highlights

- 110-year long series of wood-chemistry to understand drought-induced dieback
- Declining trees showed lower growth and higher minimum wood density than non-declining trees
- Alterations in wood nutrient concentrations are coherent with hydraulic failure hypothesis
- Mn, Ca:Mn and P:Mn rings content may serve as early-warning signals of dieback

1 *Science of the Total Environment*

2

3 *Research Article*

4

5 **Long-term nutrient imbalances linked to drought-triggered forest**

6 **dieback**

7

8 Andrea Hevia<sup>1,2,3,a,\*</sup>, Raúl Sánchez-Salguero<sup>3,4,a</sup>, J. Julio Camarero<sup>4</sup>, José I. Querejeta<sup>5</sup>,

9 Gabriel Sangüesa-Barreda<sup>6,4</sup> and Antonio Gazol<sup>4</sup>

10

11 <sup>1</sup> Forest and Wood Technology Research Centre (CETEMAS), Pumarabule, Carbayín, s/n, 33936 Siero,  
12 Asturias, Spain

13 <sup>2</sup>Departamento de Ciencias Agroforestales, Universidad de Huelva, Crta. Palos-La Rábida s/n. 21819  
14 Palos de la Frontera, Spain

15 <sup>3</sup>Dept. Sistemas Físicos, Químicos y Naturales, Universidad Pablo de Olavide, Crta. Utrera km. 1, 41013  
16 Sevilla, Spain

17 <sup>4</sup>Instituto Pirenaico de Ecología (IPE-CSIC), Avda. Montañana 1005, 50192 Zaragoza, Spain

18 <sup>5</sup>Centro de Edafología y Biología Aplicada del Segura (CEBAS-CSIC), Campus Universitario de  
19 Espinardo, PO Box 164, 30100 Murcia, Spain

20 <sup>6</sup>Depto. Ciencias Agroforestales, iUFOR-Universidad de Valladolid, Campus Duques de Soria, 42004  
21 Soria, Spain

22

23

24

25 <sup>a</sup>A. Hevia and R. Sánchez-Salguero contributed equally to this work and should be considered joint first  
26 authors.

27

28

29

30

\*Corresponding author:

31

Dr. Andrea Hevia

32

Departamento de Ciencias Agroforestales,

33

Universidad de Huelva,

34

Crta. Palos-La Rábida s/n. 21819 Palos de la Frontera

35

Huelva, Spain

36

E-mail: [aheviacabal@gmail.com](mailto:aheviacabal@gmail.com)

37

38 **Abstract**

39 Drought-induced forest dieback is causing reductions in productivity, increasing tree  
40 mortality and impairing terrestrial carbon uptake worldwide. However, the role played by  
41 long-term nutrient imbalances during drought-induced dieback is still unknown. To  
42 improve our knowledge on the relationships between dieback and nutrient imbalances,  
43 we analysed wood anatomical traits (tree-ring width and wood density), soil properties  
44 and long-term chemical information in tree-ring wood (1900-2010) by non-destructive  
45 Micro X-ray fluorescence ( $\mu$ XRF) and destructive (ICP-OES) techniques. We studied  
46 two major European conifers with ongoing drought-induced dieback in mesic (*Abies*  
47 *alba*, silver fir) and xeric (*Pinus sylvestris*, Scots pine) sites. In each site we compared  
48 coexisting declining (D) and non-declining (ND) trees. We used dendrochronology and  
49 generalized additive and linear mixed models to analyse trends in tree-ring nutrients and  
50 their relationships with wood traits. The D trees presented lower growth and higher  
51 minimum wood density than ND trees, corresponding to a smaller lumen area of  
52 earlywood tracheids and thus a lower theoretical hydraulic conductivity. These  
53 differences in growth and wood-anatomy were more marked in silver fir than in Scots  
54 pine. Moreover, most of the chemical elements showed contrasting concentrations in D  
55 than in ND trees during the last two-five decades (e.g., Mn, K and Mg), whilst Ca and  
56 Na increased in the sapwood of ND trees. The Mn concentrations, and related ratios  
57 (Ca:Mn, Mn:Al and P:Mn) showed the highest differences between D and ND trees for  
58 both tree species. These findings suggest that a reduced hydraulic conductivity,  
59 consistent with hydraulic impairment, is affecting the use of P in D trees, making them  
60 more prone to drought-induced damage. The retrospective quantifications of Mn ratios  
61 may be used as early-warning signals of impending dieback.

62

63 **Keywords:** *Abies alba*, *Pinus sylvestris*, dendrochemistry, wood density, X-ray  
64 fluorescence, Itrax, ICP-OES

65

## 66 **1. Introduction**

67 Forest dieback episodes in response to severe droughts have been observed worldwide  
68 in diverse biome types (Allen et al., 2010). Since droughts are expected to last longer  
69 and be more severe as climate warms, forest ecologists and managers are increasingly  
70 concerned about the prevalence of such dieback episodes under more arid conditions  
71 (Anderegg et al., 2015). Dieback often precedes high tree mortality and both processes  
72 are characterized by increased crown transparency and leaf shedding, decreased forest  
73 productivity, reduced radial-growth rates and increased tree mortality rates, among other  
74 symptoms (e.g., Bréda et al., 2006). Forest dieback is a complex phenomenon where  
75 several drivers may interact in addition to drought, including nutrient availability and  
76 biotic stress factors (Camarero et al., 2015; Gazol et al., 2018; Manion, 1991; Sangüesa-  
77 Barreda et al., 2015).

78 Two main physiological mechanisms (non-mutually exclusive) have been  
79 proposed to explain drought-induced dieback: hydraulic failure and carbon starvation  
80 (e.g., McDowell et al., 2008). Retrospective analyses based on tree-ring variables  
81 (width, anatomy and wood density, C and O isotope discrimination) used as surrogates  
82 of tree growth and hydraulic conductivity and water use, allow inferring the relative  
83 importance of these two major mechanisms involved in dieback processes (e.g.,  
84 Colangelo et al., 2017; Dalla-Salda et al., 2009; Pellizzari et al., 2016; Sevanto et al.,  
85 2014). Both mechanisms are linked but, nowadays, hydraulic failure seems to be  
86 involved in most cases concerning gymnosperms subjected to severe and lasting  
87 droughts (Adams et al., 2017). However, other potential mechanisms driving forest  
88 dieback, such as diminished nutrient availability and uptake remain understudied  
89 (Gessler et al., 2017; Salazar-Tortosa et al., 2018).

90 Drought reduces growth and sap flow, decreases C uptake by restricting gas  
91 exchange through stomata and increasing relative respiration costs and, as a result, may  
92 uncouple growth from photosynthesis (Hsiao, 1973; Muller et al., 2011). Drought also  
93 constrains the availability of nutrients by reducing nutrient diffusion and mass flow in  
94 soil, and by impairing root hydraulic conductivity and nutrients uptake from the soil.  
95 Thus, such decrease in nutrient availability may reduce photosynthesis rates and  
96 contribute to forest dieback (St. Clair et al., 2008), particularly in species following a  
97 conservative water-use strategy such as gymnosperms (Irvine et al., 1998; Salazar-  
98 Tortosa et al., 2018). In gymnosperms, where dieback is a long-term process  
99 characterized by lasting and low radial-growth rates of declining trees prior to tree death  
100 (Cailleret et al., 2017), nutrient imbalances (i.e., the inability of trees to absorb and  
101 retain certain nutrients) could contribute to explain dieback (Gessler et al., 2017;  
102 Szczepkowski and Nicewicz, 2008).

103 In forests where conspecific individuals show different growth and vigor  
104 responses to drought stress, the most vulnerable trees would be expected to show lower  
105 growth rates due to lower soil nutrient uptake rates (Gessler et al., 2017; McDowell et  
106 al., 2008; Timofeeva et al., 2017). However, the opposite is also possible since trees  
107 acclimated to high nutrient supply could grow more and produce wider xylem conduits  
108 making them prone to drought-induced cavitation (Levanic et al., 2011; Voltas et al.,  
109 2013). A retrospective approach could help to elucidate the role of nutrient imbalances  
110 during drought-induced dieback in relation to the two major dieback mechanisms  
111 proposed. Therefore, novel approaches to retrospectively quantify long-term changes of  
112 nutrients in wood rings are needed.

113 Nutrient imbalances in tree tissues (wood, foliage) have been previously related  
114 to forest dieback (e.g., Duchesne et al., 2002; Rozas and Sampedro, 2013). Such

115 imbalances are known to increase the long-term tree sensitivity to drought (Helama et  
116 al., 2009; Horsley et al., 2000). Essential nutrients (Ca, K, P, Mn, N) play relevant roles  
117 in tree functioning (water uptake, stomatal conductance, cell division and cell-wall  
118 synthesis), so trees may modify their use and allocation in response to drought (Lautner  
119 and Fromm, 2010; Schlesinger et al., 2016; Yoshimura et al., 2016). Nonetheless,  
120 studies on the interactions between drought-induced dieback and long-term nutrition  
121 imbalances are still scarce (but see Gessler et al., 2004, 2017).

122         Here, we used dendrochemistry, i.e., the study of nutrients in annually dated  
123 tree-rings (cf. Smith et al., 2014), to assess how nutrient imbalances may contribute to  
124 drought-induced dieback. We compared the long-term wood nutrient relative  
125 concentrations in coexisting declining (hereafter D trees) vs. non-declining (hereafter  
126 ND trees) individuals of two gymnosperms subjected to recent drought-induced  
127 dieback. These two conifers are very important European tree species and inhabit  
128 climatically contrasting sites: silver fir (*Abies alba* Mill.) was studied in a wet-cool or  
129 mesic site, and Scots pine (*Pinus sylvestris* L.) was studied in a dry-continental or xeric  
130 site (see more details in Camarero et al., 2011, 2015; Gazol and Camarero, 2016). We  
131 also looked for early signals in the wood nutrient annual series since similar analyses  
132 based on tree-ring width (Cailleret et al., 2017; Camarero et al., 2015) or tracheid lumen  
133 area (Pellizzari et al., 2016) found differences between coexisting D and ND trees  
134 several decades before the dieback started.

135         We hypothesize that D trees were more vulnerable to drought due to long-term  
136 nutrient imbalances. Specifically, we compare wood anatomical traits (tree-ring width  
137 and wood density) and nutrient concentrations (e.g., Ca, Mn, K, Mg, Na and Zn) in  
138 coexisting D and ND trees to determine if drought-related dieback is linked by long-  
139 term nutrient imbalances. We expect that: (i) D trees will show lower growth rates than

140 ND trees; (ii) D trees will have a denser earlywood (higher minimum wood density)  
141 than ND trees because the former will produce tracheids with smaller lumen diameter,  
142 i.e. having a lower theoretical hydraulic conductivity, than the latter (cf. Pellizzari et al.,  
143 2016); and (iii) D trees will show decreases in hydraulic conductivity and growth linked  
144 to long-term nutrient imbalances. Investigating the role of nutrient imbalances in  
145 drought-induced dieback processes will improve our understanding of which forests,  
146 tree species or individual trees will be the most vulnerable to drought damage and  
147 reduction in carbon uptake and productivity (William et al., 2015).

148

## 149 **2. Material and methods**

### 150 *2.1. Study sites and tree species*

151 We selected two sites in northeastern Spain subjected to wet and cool conditions (silver  
152 fir, *A. alba*) and continental and dry conditions (Scots pine, *P. sylvestris*) (see Table A1  
153 in Appendix A). These sites were characterized by presenting abundant defoliated,  
154 dying or recently dead trees affected by different severe droughts. The percentage of  
155 radial growth reduction relative to background levels was applied to identify drought-  
156 induced abrupt decreases of growth following Camarero et al. (2018). The most abrupt  
157 growth reductions occurred in: 1986, 1994-1995 and 2012 in the case of silver fir; early  
158 1980s, 1994-1995, 1999, 2005 and 2012 in the case of Scots pine (see Camarero et al.,  
159 2011, 2015, 2018). Climatic data showed temperature rises in the region during the  
160 1940s and 1980s (Camarero et al., 2011). Annual precipitation increased during the  
161 1970s, whereas it decreased in the 1980s and 1990s (Camarero et al., 2011). The two  
162 study conifers show isohydric regulation of their water status by avoiding hydraulic  
163 failure through rapid stomatal closure (Bréda et al., 2006). The soil in both sites was

164 neutral to slightly basic in pH, although soils are deeper and more developed at the  
165 silver fir than at the Scots pine site (Gazol et al., 2018; see also Tables A1 and A5).

166

## 167 *2.2. Field sampling and dendrochronological data*

168 At each study site, 38 trees of each species were selected in an area between 0.5 and 2.0  
169 ha, with target trees located at least 10 m apart from each other (Camarero et al., 2015;  
170 Gazol et al., 2018). We measured size variables (DBH, diameter at breast height  
171 measured at 1.3 m; H, total tree height) and defoliation status in the selected trees to  
172 characterize the dieback pattern. Tree defoliation was estimated as the percentage of  
173 crown defoliation using binoculars with a reference tree with the maximum amount of  
174 foliage at each site (Dobbertin, 2005), and two vigor classes were differentiated: ND  
175 trees (crown defoliation < 50%) and D trees (crown defoliation  $\geq$  50%). This has been  
176 shown as a robust criterion to differentiate ND from D trees (see Camarero et al., 2015)  
177 (Table A1).

178 We used dendrochronology to retrospectively characterize growth and wood  
179 density of trees (Fritts, 2001). Radial growth was measured by extracting two radial  
180 cores per tree at 1.3 m using a 5-mm Pressler increment borer. Sampling was done in  
181 late 2012. We measured the length of the sapwood in the collected cores in the field;  
182 and for silver fir we applied stain (bromocresol green) to distinguish the sapwood  
183 (Table A2). Wood samples were sanded until tree-rings were visible and then visually  
184 cross-dated. Tree-ring width (hereafter RW) was measured to the nearest 0.01 mm using  
185 a binocular microscope and a LINTAB measuring device (Rinntech, Heidelberg,  
186 Germany). The accuracy of visual cross-dating and ring-width measurements was  
187 checked using the COFECHA program, which calculates moving correlations between  
188 each individual tree-ring series and the mean site series (Holmes, 1983).

189

190 *2.3. Tree-ring traits and dendrochemical non-destructive analyses measured at annual*  
191 *scale*

192 Since dendrochemical studies require fewer sampled trees than classical  
193 dendrochronological studies (cf. Balouet and Chalot, 2015), we randomly selected five  
194 trees per vigor class (D vs. ND trees) in each species (Table A1). We selected trees with  
195 high correlation with the mean ring-width site chronology, a low frequency of missing  
196 rings, no tree-ring sequences with widths narrower than 0.1 mm to ensure enough  
197 material to resolve chemical compounds at annual resolution, no significant growth  
198 suppressions and releases and no scars or reaction wood (see Hevia et al., 2018). These  
199 selected trees were cored at 1.3 m using a 10-mm Pressler increment borer. The cores  
200 were mounted and thin laths of around  $1.0 \pm 0.02$  mm thickness were cut transversely  
201 using a high-precision twin-bladed saw. These thin laths were kept under controlled  
202 conditions (temperature and humidity) before X-ray analysis in an Itrax Multiscanner  
203 (Cox Analytical Systems, Sweden) at the laboratory of CETEMAS (Siero, Asturias,  
204 Spain). Itrax was operated at 30 KV and 50 mA with a Cu-tube, and samples were  
205 exposed to the X-ray beam for 10 seconds at each measurement point in radial direction  
206 (50- $\mu$ m step size). Count rates of fluorescent photons of elements (for chemical  
207 characterization) and a radiographic greyscale image (for wood density) in each  
208 measurement point of each sample were obtained. Peaks in the micro X-ray  
209 Fluorescence ( $\mu$ XRF) spectrum were assigned to specific elements using the Q-spec  
210 software (Cox Analytical Systems, Sweden), producing relative concentrations (count  
211 rates of fluorescent photons) (e.g., Croudace et al., 2006) of those elements detected  
212 within the wood structure for every analyzed point. The same chemical elements were  
213 detected for both species. The radiographic images were cross-dated with previously  
214 built chronologies in each site to assign the element specific count rates of each annual

215 ring. For this purpose, tree-ring-boundaries were defined on each radiographic image  
216 using WinDendro<sup>TM</sup> (Regent Instruments, Canada). In addition, tree-ring width (RW),  
217 earlywood width (EW), latewood width (LW), earlywood proportion (PEW) , latewood  
218 proportion (PLW) , mean ring density (RD), earlywood density (ED), latewood density  
219 (LD), maximum (MXD) and minimum wood densities (MND) were extracted (see  
220 Table A2) from the radiographic images after calibrating the greyscale intensities to  
221 wood densities using a light calibration curve derived from a calibration wedge  
222 (Schweingruber, 1996). Average annual time series for each tree were produced  
223 considering the following detected elements: magnesium (Mg), calcium (Ca), potassium  
224 (K), phosphorus (P), sulphur (S), strontium (Sr), aluminium (Al), manganese (Mn) and  
225 zinc (Zn). Lastly, seven meaningful molar ratios were also explored: Al:Ca, Ca:Mn,  
226 K:Ca, Mg:Mn, Mn:Al, P:Mn and Sr:Ca (e.g., Hevia et al., 2018; Houle et al., 2007;  
227 Kuang et al., 2008; Scharnweber et al., 2016; Silkin and Ekimova, 2012).

228

#### 229 *2.4. Destructive wood nutrient analyses measured at decadal scale*

230 To compare the changes in tree-ring nutrients by non-destructive  $\mu$ XRF and destructive  
231 direct methods, individual cores were also analyzed for element (Al, Ca, K, Mg, Mn,  
232 Na, P, S, Sr, Zn) concentrations by inductively coupled plasma optical emission  
233 spectrometry (ICP-OES, Thermo Elemental Iris Intrepid II XDL, Franklin, MA, USA)  
234 after a microwave-assisted digestion with HNO<sub>3</sub>:H<sub>2</sub>O<sub>2</sub> (4:1, v:v) in the Ionomics  
235 laboratory at CEBAS-CSIC (Murcia, Spain). The remaining wood from laths of the  
236 same trees selected for dendrochemistry were carefully separated in decadal wood  
237 segments for the period 1900-2010. Decadal pools were obtained for ND and D trees of  
238 each species. Then, 10-year bulk samples of coarse wood were ground and  
239 homogenized to a fine powder using a ball mill (Retsch MM301, Haan, Germany).

240 Wood N mass-based concentration (%) was measured with an elemental analyser  
241 (Elementar VarioMAX N/CM, Hanau, Germany). We also calculated N:P, N:K and P:K  
242 ratios to determine (i) whether the D and ND trees show different long-term trends and  
243 (ii) whether each of the two studied species presented significant effects on long-term  
244 nutrient imbalances by analyzing the data of all elements and elements' ratios together.

245

#### 246 *2.5. Soil traits and nutrient availability*

247 For each sampled tree, we collected three top soil samples from the uppermost 25 cm  
248 close to the trunk (< 50 cm in distance) below the canopy of D and ND trees. Prior to  
249 collection of the soil samples the litter layer was removed carefully. Soil C and N  
250 concentrations and the C:N ratio were determined with an elemental analyzer  
251 (Elementar VarioMAX N:CM, Hanau, Germany) (Table A1). Soil samples were then  
252 sieved at 2 mm and air-dried to measure soil pH in distilled water. Soil nutrients Al, Ca,  
253 K, Mg, Na, P, S and Zn) were measured by ICP-OES (see Table A5).

254

#### 255 *2.6. Data analyses*

256 To constrain high variance and differences of concentration (element specific count  
257 rates), tree-ring  $\mu$ XRF series were normalized to their mean and standard deviation (Z-  
258 scores, i.e., the mean was subtracted from each value and divided by the standard  
259 deviation). Z-scores were calculated for each series of element measurements per  
260 sampled tree, and then averaged into a mean series of each element. Each mean series  
261 included at least 5 trees for any given year for the 1900-2010 period (years after 2010  
262 were deleted to eliminate potential edge effects due to diffraction at the sample edges in  
263 Itrax (cf. Scharnweber et al., 2016)). Decadal values of elements concentrations were  
264 obtained by destructive methods (ICP-OES, pooled tree-rings) (see Figs. 3 and A1).

265 In order to assess the common variance among time series of element  
266 concentrations (annual resolution,  $\mu$ XRF), and possible inter-correlations between the  
267 elements and wood traits (RW, MXD and MND), we used Spearman correlation  
268 analysis because some variables (e.g., MXD) did not follow normal distributions.  
269 Values of wood traits and element concentrations were compared between D and ND  
270 trees using the non-parametric Mann-Whitney *U*-test. To test within- and between- year  
271 variability in tree-ring elements between D and ND trees, Generalized Additive Mixed  
272 Models (GAMM; Wood, 2006) were fitted at tree level since these models allow  
273 characterizing non-linear trends that vary at different time scales. To assess if the  
274 chemical elements presented different trends between D and ND trees and within each  
275 species we proposed five different models: (i) containing only the intercept; (ii)  
276 considering only tree vigor; (iii) considering only calendar year; (iv) considering  
277 calendar year and tree vigor; and (v) considering calendar year, tree vigor and their  
278 interaction. The last model indicates the presence of different temporal trajectories in  
279 chemical elements between individuals. Tree identity was considered random factor  
280 since each tree represents repeated measures over the same individual. We also included  
281 the first-order autocorrelation structure (AR1()) to account of the dependency of  
282 chemical composition in year *t* of year *t-1*. We ranked the five potential models  
283 according to the second-order Akaike information criterion (AICc). The model showing  
284 the lowest AICc value and largest Akaike weight ( $W_i$ , relative probability quantifying if  
285 the selected model is the best one) was selected as the best model.

286 To study the influence of vigor class and wood traits on annual tree-ring  
287 elements ( $\mu$ XRF), we used Linear Mixed-Effects models (LME; Pinheiro and Bates,  
288 2000) at the tree scale. Specifically, we proposed a model in which the vigor class (D  
289 vs. ND) and individual wood traits (tree-ring widths and wood densities) were used as

290 fixed factors, whereas tree identity was regarded as random factor. Separate models  
291 were constructed for each element based on annual Z-scores data. To identify the set of  
292 predictors that better explained the observed patterns for each element, we used a multi-  
293 model inference approach based on information theory (Burnham and Anderson, 2002).  
294 The model with the lowest AICc value and largest Akaike weight ( $W_i$ ) was considered  
295 as the best (most parsimonious) model. We also calculated the  $\Delta AICc$  (AICc  
296 differences between each model and the best model) to rank competing models. For  
297 each explanatory variable, we calculated its relative importance across all the models.  
298 To quantify the strength of the model, we calculated a pseudo- $R^2$  (Nakagawa and  
299 Schielzeth, 2013). Residuals of the models were checked for normality,  
300 homoscedasticity and temporal autocorrelation. Lastly, to elucidate potential influences  
301 of outliers, we evaluated the fit of the model by graphical examination of the residuals  
302 and the fitted values.

303 All statistical analyses were performed in the R environment (R Development  
304 Core Team, 2018). Tree-ring chronology building and related analyses were done using  
305 the package *dplR* (Bunn et al., 2018). The *gamm* function of the *mgcv* package was used  
306 to fit the GAMM (Wood, 2006), and the *lme* function of the *nlme* package was used to  
307 fit the LMEs (Pinheiro et al., 2014) models. The *MuMIn* package was used to perform  
308 the multi-model selection (Barton, 2012).

309

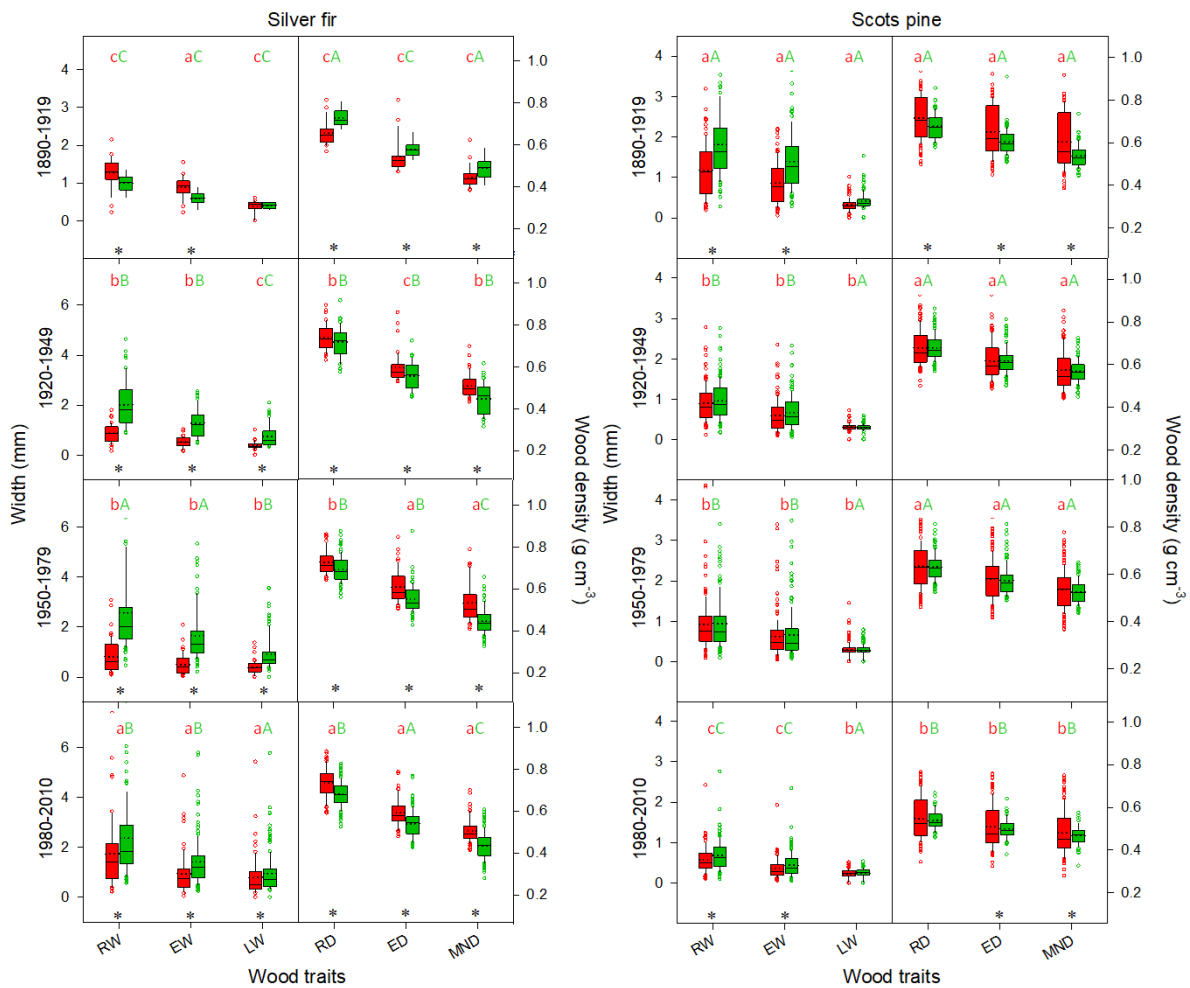
### 310 **3. Results**

#### 311 *3.1. Radial growth and wood density*

312 The D trees showed significantly ( $P < 0.05$ ) lower DBH and sapwood proportion (PSW)  
313 than ND trees for both species (Tables A1 and A2). D trees also presented narrower  
314 rings than ND trees (Figs. 1 and A2; Table A2) after 1950s. This reduction in growth of

315 D trees as compared to ND trees corresponded to lower EW values and this difference  
 316 was amplified after the 1950s in silver fir and after the 1980s in Scots pine (Fig. 1;  
 317 Table A2).

318 Wood density traits significantly differed between vigor classes in both tree  
 319 species, with higher values (RD, ED and MND) in D than in ND trees after the 1980s  
 320 (Figs. 1 and A2; Table A2). In silver fir a clear divergence in MND was observed with  
 321 higher values for D than for ND trees since the 1990s (Fig. A2).



322 **Figure 1.** Temporal variability in the wood traits (RW, tree-ring width; EW, earlywood  
 323 width; LW, latewood width; RD, ring density; ED, earlywood density; MND, minimum  
 324 wood density) for the periods 1890-1919, 1920-1949, 1950-1979 and 1980-2010 in D  
 325 (declining, red colour) and ND (non-declining, green colour) silver fir (*Abies alba*, left  
 326 column) and Scots pine (*Pinus sylvestris*, right column) trees. Box-plots present median  
 327 (horizontal black line), mean values (horizontal dotted black line), outliers (dots) and  
 328

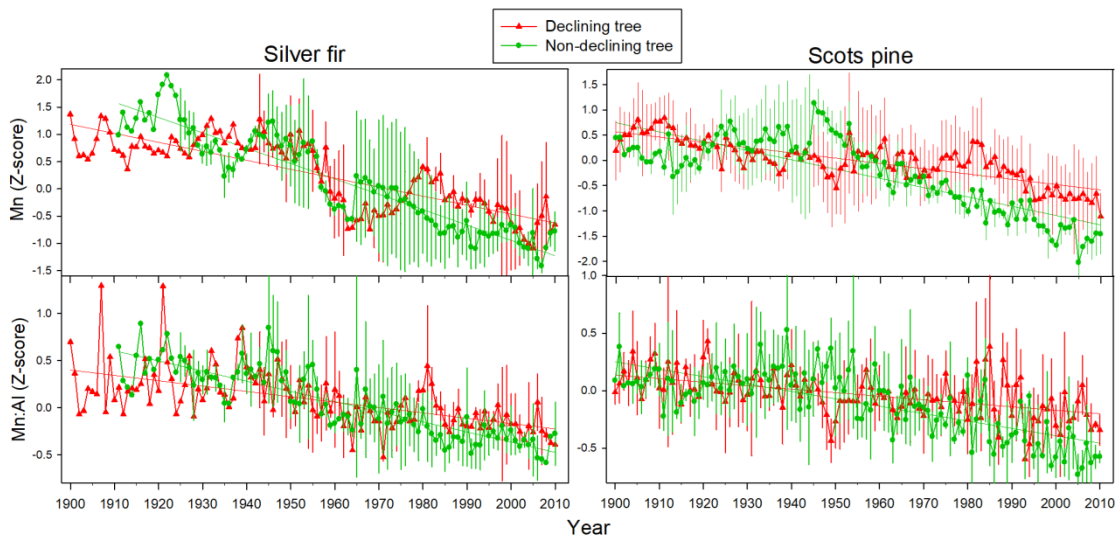
329 standard deviation (black bars). Asterisks indicate significant ( $P < 0.05$ ) differences in  
330 wood traits between vigor status for each period; and uppercase and capital letters mean  
331 differences within status among the four periods according to Mann-Whitney  $U$ -test.

332

### 333 *3.2. Long-term wood chemistry patterns*

334 D and ND trees showed similar long-term trends and high-frequency patterns of tree-  
335 ring chemical elements within each species (Figs. 2, 3 and A3). According to the fitted  
336 GAMMs, the explained variability for chemical elements in silver fir and Scots pine  
337 was strongly variable depending on the element considered (Tables A3 and A4).  
338 Negative long-term trends were observed for Ca and Mn in both tree species, with  
339 differences between D and ND trees during the last decades (Figs. 2, 3 and 4). In silver  
340 fir, the Ca concentration started to decrease in the 1960s for D trees, and in the 1990s  
341 for ND trees (Fig. 3). However, Scots pine presented a marked decreasing trend for Ca  
342 after the dry 1980s regardless the vigor class. In contrast, the Mn trend decreased before  
343 in ND trees than D trees in both species, starting in the 1970s in silver fir and in the  
344 1950s in Scots pine, with a lightly increasing trend in the D trees after 1980s for both  
345 tree species (Figs. 2 and 4).

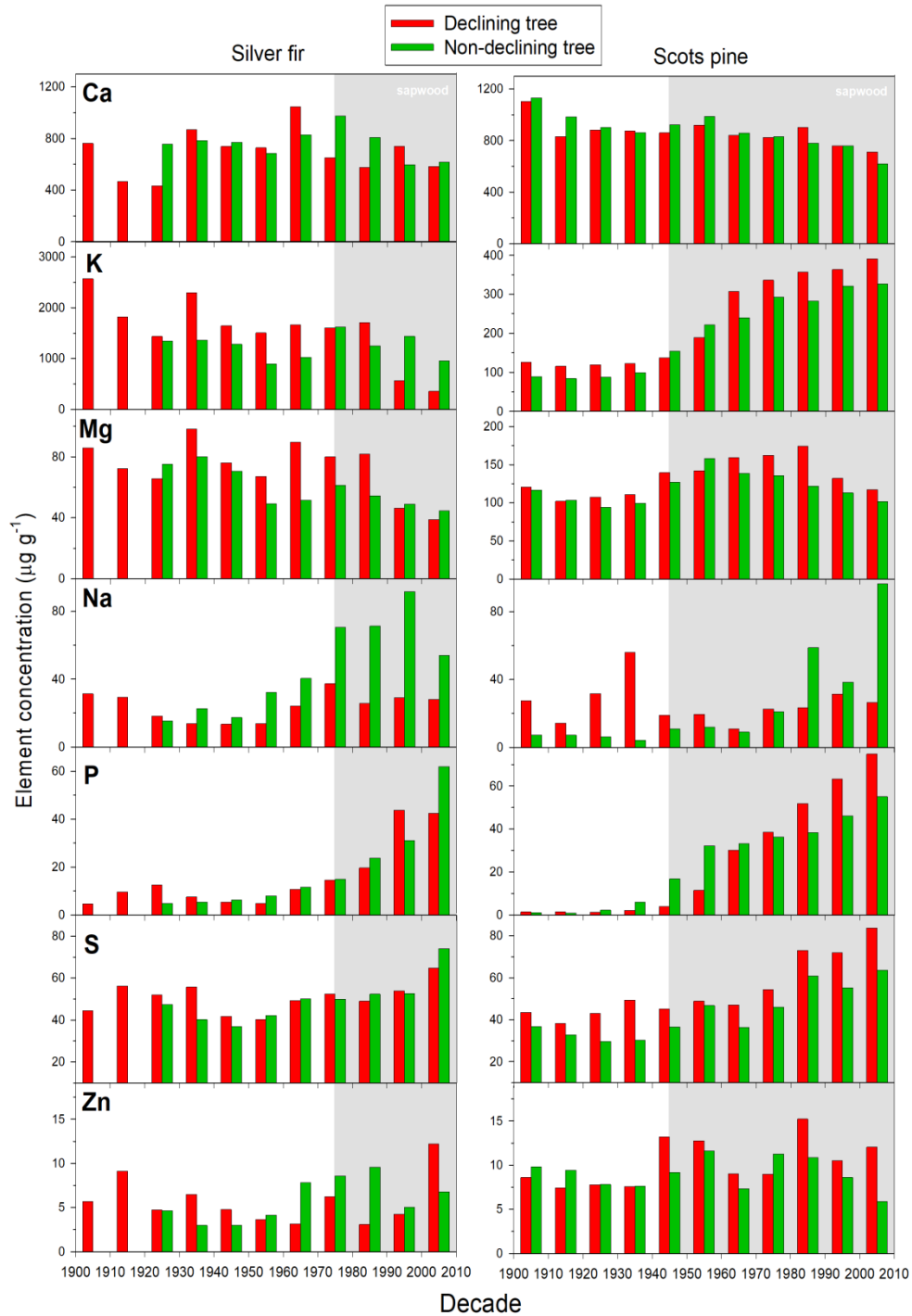
346         Conversely, Na presented a positive trend for both species and tree classes in the  
347 long-term (Fig. 3; Tables 1 and A3). K also presented sharp long-term changes,  
348 decreasing in silver fir but increasing in Scots pine at the heartwood-sapwood boundary  
349 for both D and ND trees (Fig. 3). In this respect, mean heartwood/sapwood transitions  
350 were dated approximately in 1975 and 1945 for silver fir and Scots pine, respectively.



351  
 352 **Figure 2.** Annual values of element relative concentration of selected elements (Mn and  
 353 molar ratio Mn:Al) obtained through  $\mu$ XRF of declining (D, red dots and lines) and  
 354 non-declining (ND, green dots and lines) trees in silver fir (left column) and Scots pine  
 355 (right column). Values are means Z-scores  $\pm$  SD.

356

357 Mg, Zn and Al did not show clear differences between D and ND trees for silver  
 358 fir, in contrast to Scots pine which presented differences for P and those elements  
 359 during the 20<sup>th</sup> century (Table A3; Fig. 3). During the last decades, K, Mg, Mn and Zn  
 360 increased in D Scots pine trees, whereas Ca and Na increased in ND trees (Fig. 3).  
 361 Lastly, P and S showed different trends between species after 1980s (increasing values  
 362 in ND trees in silver fir and D trees in Scots pine, respectively; see Table A3 and Fig.  
 363 3).

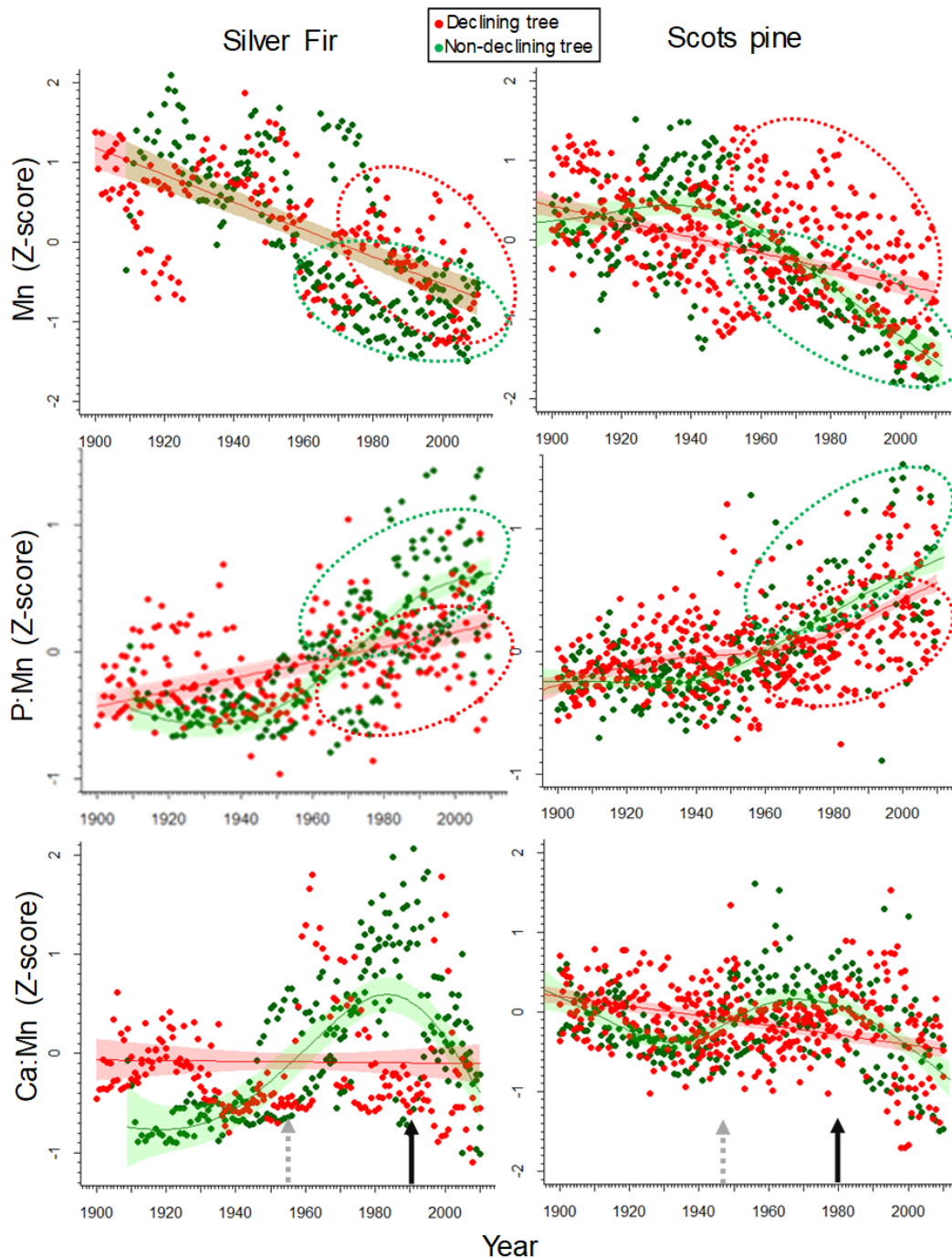


364

365 **Figure 3.** Decadal values of elements concentrations in wood (ICP-OES,  $\mu\text{g g}^{-1}$ ). Data  
 366 are presented for declining (D, red bars) and non-declining (ND, green bars) silver fir  
 367 (left column) and Scots pine (right column) trees. The grey boxes include the decades  
 368 corresponding to the mean sapwood for the sampled trees (35 years for silver fir and 45  
 369 years for Scots pine).

370

371 The GAMMs showed that Mn in Scots pine and its molar ratios (Ca:Mn, Mn:Al,  
 372 Mg:Mn and P:Mn) and also P for both species were the best indicators of long-term  
 373 nutrient divergences between D and ND trees in both species (Table A3; Figs.4, A3 and  
 374 A4). The most clear difference between D and ND trees was observed in Ca:Mn and  
 375 P:Mn (decrease in D) and Mn:Al (increase in D) (Figs. 4 and A4; Table A3).

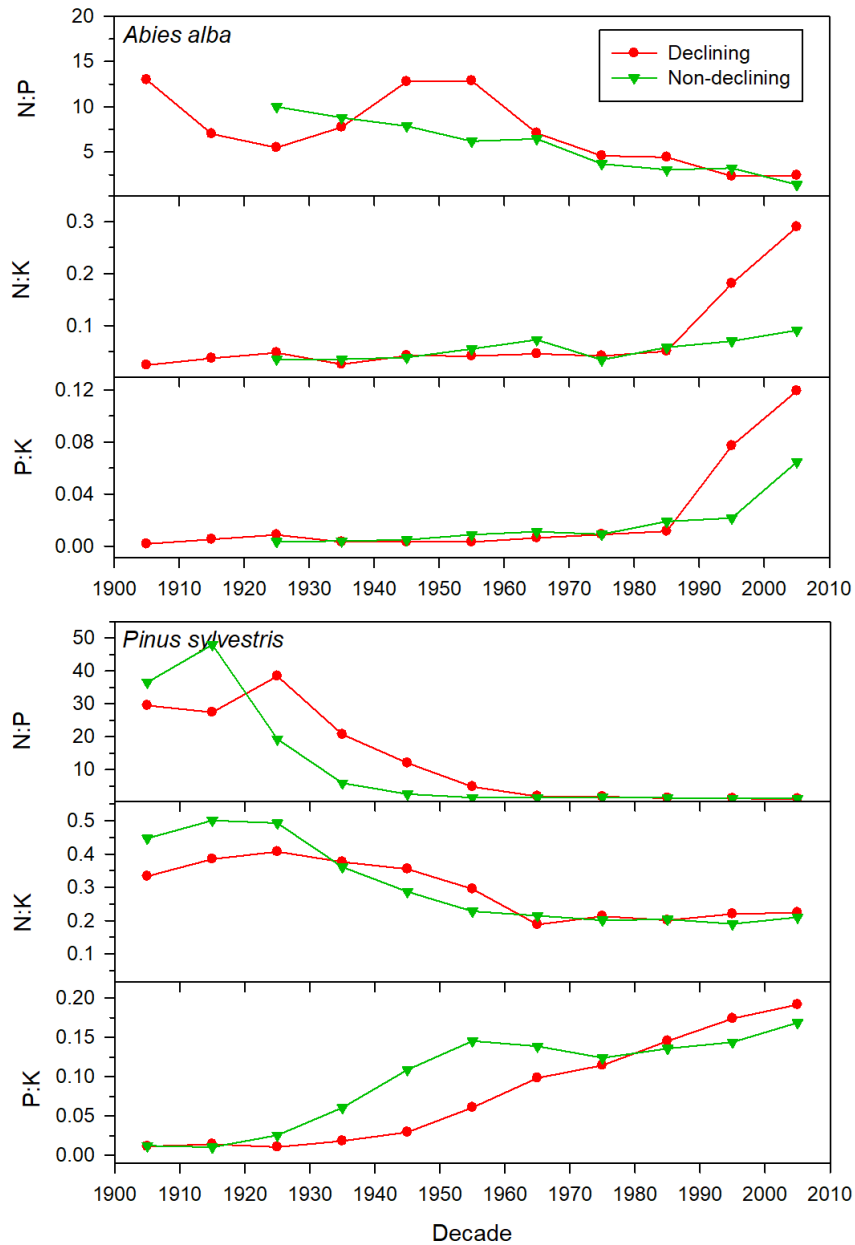


376  
 377 **Figure 4.** Observed (points) and fitted (lines with confidence intervals) long-term trends  
 378 in Z-scores of selected elements obtained through  $\mu$ XRF of declining (D, red dots and

379 lines) and non-declining (ND, green dots and lines) silver fir (left column) and Scots  
380 pine (right column) trees. Generalized Additive Mixed Models (GAMM) were used to  
381 characterize the changes in analysed elements (see Table A3). Vertical grey and black  
382 arrows indicate nutrient (i.e., molar ratio Ca:Mn) and tree growth (see Fig. A2, cf.  
383 Camarero et al., 2015) divergences in trends between D and ND trees, respectively.  
384 Ellipses (dashed lines) include the 95% data for each tree status after nutrient (Mn and  
385 P:Mn) divergences (see vertical grey arrow).

386

387           The N:P and N:K ratios showed similar trends in D than in ND trees, but the  
388 N:K and P:K ratios started diverging between D and ND trees in the 1980s, markedly  
389 for silver fir, and slightly for Scots pine (Fig. 5).



390

391 **Figure 5.** Decadal values of stoichiometric ratios (N:P, N:K and P:K) in wood obtained  
 392 from ICP-OES analyses. Data are presented for declining (D, red lines) and non-  
 393 declining (ND, green lines) silver fir (*Abies alba*, upper plots) and Scots pine (*Pinus*  
 394 *sylvestris*, lower plots) trees.

395 **Table 1.** Model selection table of Linear Mixed-Effects models (LME) fitted to wood  
396 nutrients data and wood traits trends in silver fir (*Abies alba*) and Scots pine (*Pinus sylvestris*)  
397 for the 1900–2010 period. The model showing the lowest Akaike Information Criteria (AICc)  
398 was selected as the best model. For each model, we show the selected variables, the most  
399 parsimonious model, which reduced  $\Delta\text{AICc}$ , and the model Akaike weight ( $W_i$ ) or probability  
400 that the selected model is the best one, and coefficients associated to each variable and their  
401 significance levels (\* $P < 0.05$ ; \*\* $P < 0.01$ ).

Tree	Variable	ED†	ED*S	EW	EW*S	LD	LD*S	LW	LW*S	S	Wi	$\Delta\text{AICc}$	R <sup>2</sup>
<i>Abies alba</i>	Mg	-1.01	2.95**			-2.60*				-2.98*	0.21	1.26	0.04
	Al			1.41	-3.06**	0.99	2.82**	-1.71		-2.26	0.16	0.51	0.08
	P					1.68					0.06	0.02	0.01
	S			-1.63							0.05	0.22	0.01
	K										0.11	0.75	0
	Ca			-3.33**	1.55	-4.14**	2.41*	-4.25**	1.95	-2.83*	0.14	0.20	0.06
	Mn	2.90**	-1.62	-2.65**				-2.62**	2.34*		0.10	0.56	0.06
	Zn										0.11	1.33	0
	Sr	-4.52**		2.71**		-5.35**		-2.94**	2.51*	-1.30	0.20	1.73	0.16
	Al:Ca	-2.87**								-1.89	0.07	0.57	0.05
	Ca:Mn	-4.74**	-4.20**	-2.18*	3.36**	-1.50	1.55			-4.42*	0.17	0.13	0.06
	K:Ca			1.95		1.74		1.65			0.06	0.66	0.01
	Mg:Mn			2.20*		-2.42*					0.08	0.74	0.03
	Mn:Al	3.23**	-2.10*	-2.05*						1.94	0.09	0.47	0.07
	P:Mn	-2.40**		2.11*							0.08	0.90	0.03
Sr:Ca	-1.12	-3.71**	2.74**					2.45*	-1.71	3.68*	0.13	0.35	0.06
<i>Pinus sylvestris</i>	Mg										0.15	1.68	0
	Al					-2.38*					0.13	1.21	0.01
	P					-0.93	-2.27*	1.73		2.57*	0.09	0.73	0.04
	S					-2.89**					0.05	0.26	0.02
	K	-2.37*				-5.82**					0.19	1.51	0.03
	Ca	-4.15**	2.43*			-5.71**	-3.34**	-2.70**		0.28	0.36	1.81	0.05
	Mn	6.24**									0.11	0.73	0.04
	Zn					1.79					0.13	1.16	0.01
	Sr	-4.87**		1.63		-3.13**					0.16	0.61	0.23
	Al:Ca	1.66	2.66**			-2.95**					0.14	0.14	0.05
	Ca:Mn	-5.32**				-3.75**		-1.85			0.11	0.45	0.21
	K:Ca	-2.14*				2.63**	2.13*			-0.30	0.06	0.03	0
	Mg:Mn	-4.40**	3.70*							-3.59*	0.21	1.42	0.04
	Mn:Al	5.29**	-4.32**			3.28**				4.31**	0.16	1.03	0.14
	P:Mn	-5.30**	2.47*	-2.84**						-2.33	0.14	1.52	0.12
Sr:Ca	-2.43*				3.56**		2.64**			0.20	1.68	0.01	

402 †Abbreviations: EW – earlywood width; LW – latewood width; ED – earlywood density; LD – latewood  
403 density; S – status: declining (D trees, status = 1) and non-declining (ND trees, status = 0) trees.

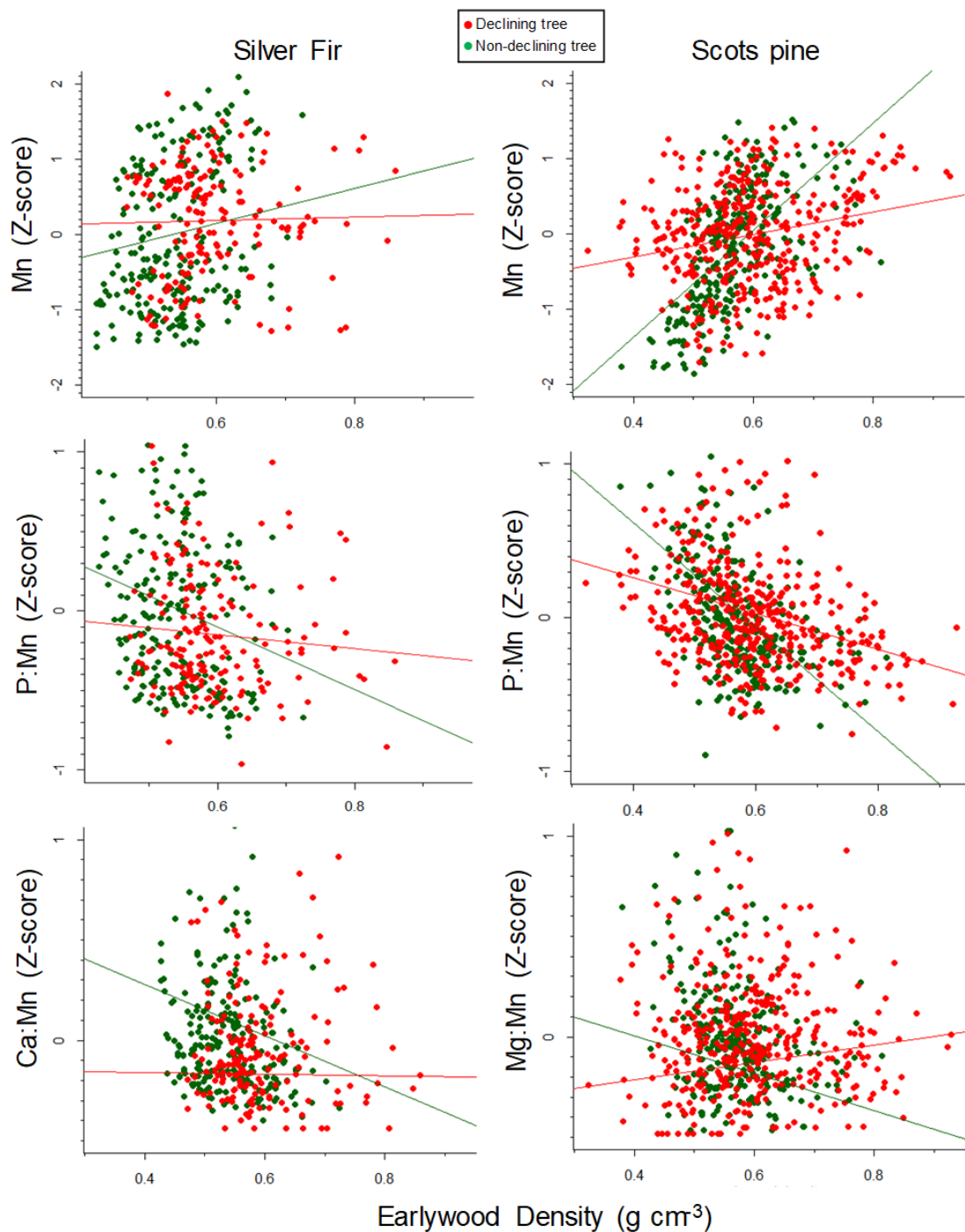
404

405

406 3.3. Associations between wood traits and tree-rings nutrients imbalances

407 We found contrasting relationships between wood traits (RW, MXD, MND) and elements  
408 (Ca, K, Mg, Mn; molar ratios Ca:Mn, P:Mn, K:Ca and Sr:Ca) depending on the vigor status in  
409 both species (Figs.6, A5 and A6; Tables 1 and A6). In silver fir, positive correlations between  
410 elements such as K, Mn and P, and variables related to maximum wood density (MXD or LD)  
411 were observed for D trees, while RW showed negative correlations with Mn, P:Mn and K:Ca  
412 (Table 1 and Fig. A5). In contrast, Scots pine showed positive correlations between  
413 earlywood density (MND or ED) and Mn, with higher values in ND than in D trees (Table 1;  
414 Figs. 6 and A5).

415 According to the LMEs, the earlywood density (ED) and width (EW) were the wood  
416 traits which accounted for most nutrient variability in silver fir and Scots pine, respectively  
417 (Table 1; Figs. 6 and A6). These models suggested that the ED, a proxy of the lumen area of  
418 earlywood tracheids and conductivity, had diverged between D and ND trees at least since the  
419 1950s in both species, and that change was linked to changes in chemical elements (Tables 1  
420 and A6; Figs. 1 and A2). The LMEs showed that Mn, Ca:Mn and Mg:Mn were suitable  
421 indicators of long-term nutrient imbalances and divergences between D and ND trees in  
422 relation to wood traits (i.e., Mn for both species, Ca:Mn for silver fir and Mg:Mn for Scots  
423 pine) (Table 1; Fig. 6). We found that P, S and K:Ca showed the highest divergences between  
424 D and ND trees in relation to latewood width (LW) in both species (Table 1). In silver fir,  
425 Mn, Al:Ca, Ca:Mn and P:Mn showed that earlywood density (ED) was the most important  
426 wood trait related to nutrient trends, with significant differences since 1980s between D and  
427 ND trees ( $F= 18.21$ ,  $P = 0.007$ ; Fig. 6 and Table 1).



428  
 429 **Figure 6.** Relationships between observed elements concentration (Z-scores of selected  
 430 elements obtained through  $\mu$ XRF) and earlywood density of declining (D, red dots and lines)  
 431 and non-declining (ND, green dots and lines) in silver fir (left column) and Scots pine (right  
 432 column) trees. Linear mixed-effects models were used to characterize the trends in the  
 433 relationships for the analysed elements (see Table 1).

434 Only D silver fir trees presented a sustained increase in ED and MND, particularly  
435 since the late 1980s (Fig. A2), in agreement with the changes in Ca, Mn and Mg  
436 concentrations (Fig. 6). Overall, the nutrient variability responded more to year-to-year  
437 variability of wood density in Scots pine than in silver fir, with minor differences between the  
438 two vigor classes (Table 1; Figs. 6 and A6).

439

### 440 *3.4. Soil chemical properties*

441 Soil nutrient concentrations presented some differences between vigor classes (Table A5). In  
442 the case of silver fir, soil contents of Al, Ca, K, Mg, Na and Zn were higher for soils sampled  
443 below D trees than below ND trees (Table A5). In the case of Scots pine, soil content of the  
444 same nutrients, except Zn, but also P and S were higher below D than below ND trees.

445

## 446 **4. Discussion**

447 Tree-ring variables are important sources of retrospective, long-term information on tree  
448 growth and vigor (e.g., Camarero et al., 2015; Carrer et al., 2018), but also an invaluable  
449 source of data about environmental changes and tree nutritional status (e.g., Hevia et al.,  
450 2018; Smith et al., 2014). Our findings provide insights into the role of long-term nutrients  
451 imbalances in the physiological mechanisms underlying the contrasting responses of tree  
452 species to forest dieback processes. We showed that long-term nutrient imbalances could  
453 contribute to dieback and growth decline. Therefore, such nutrient imbalances could be used  
454 as early-warning signals of impending tree mortality. Specifically, the reduction in growth  
455 rates and the increase of earlywood density, which indicates a loss in hydraulic conductivity,  
456 of declining trees were consistent with hydraulic impairment. This was reflected in D trees  
457 with a decrease in Na and increase in Mn concentrations relative to ND trees, as well as  
458 steeper rises in N:K and P:K ratios in younger sapwood (Fig. 5). Our findings revealed that

459 the combination of wood traits, surrogates of growth and hydraulic properties (Lachenbruch  
460 and McCulloh, 2014), and nutrient contents in wood, proxies of basic physiological functions  
461 (e.g., Fromm, 2010; Lautner and Fromm, 2010; Oddo et al., 2014), allows uncovering and  
462 monitoring dieback processes decades prior to the onset of tree growth decline, supporting the  
463 role of wood nutrients as potential early-warning signals of forest dieback.

464

#### 465 *4.1. Tree-ring growth and wood density patterns in relation to droughts*

466 Our findings agree with previous studies in which tree-ring width (Cailleret et al., 2017) or  
467 tracheid lumen area (Pellizzari et al., 2016) showed differences between D and ND trees  
468 several decades prior to tree death (Figs. 1 and A2). We found larger differences in growth  
469 rates and earlywood density between D and ND trees in silver fir than in Scots pine (see Figs.  
470 1 and A2), which could be related with the limiting xeric climate conditions of the Scots pine  
471 site, which severely constrains growth in both D and ND trees, compared to the mesic silver  
472 fir site, where decline symptoms became conspicuous in the 1980s (Camarero et al., 2015;  
473 Gazol and Camarero, 2016). Nevertheless, both species were sensitive to drought at the two  
474 studied rear-edge populations (Sánchez-Salguero et al., 2017).

475 Silver fir presented a clear divergence in growth between D and ND trees after the  
476 1980s due to the intensification of the warming trend and drought severity in the 1990s and  
477 the legacy effects of the 1985-1986 extreme drought (Camarero et al., 2011, 2015; Sangüesa-  
478 Barreda et al., 2015). Attending to a recent study showing that ND trees presented higher  
479 growth rates than D trees (Camarero et al., 2018), our results highlight the capacity of silver  
480 fir to recover after extreme droughts at long-term scales (Fig. A2; Table A2). In contrast, the  
481 reduction in growth for D trees of Scots pine in relation to ND trees started in the 1980s,  
482 which was a warm and dry decade (Pellizzari et al., 2016). Furthermore, radial growth of this  
483 species was severely impacted by successive droughts in the 1990s, 2000s and 2010s

484 suggesting a chronic drought-induced dieback in this xeric site (Camarero et al., 2015, 2018).  
485 This could explain the small differences observed between D and ND trees regarding MND  
486 (Figs. 1 and A2; Table A2).

487 Several studies have also revealed that radial growth is closely linked to intrinsic tree  
488 features such as sapwood area in conifers which affects hydraulic conductivity and stem water  
489 storage (e.g., Galván et al., 2012). Trees which produce a greater proportion of sapwood are  
490 expected to show greater radial growth (Galván et al., 2014), which concurs with our results  
491 in ND trees for both species (Table A2; Camarero et al., 2015). A hydraulic deterioration  
492 prior to the dieback onset has been associated to a chronic process for both conifers (Pellizzari  
493 et al., 2016). Probably, the decline started as a consequence of the drier conditions from the  
494 1950s onwards in both study sites, which concurs with our findings for minimum wood  
495 density (Figs. 1 and A2). During the 1980s, MND of D and ND trees started to diverge in  
496 silver fir (Fig. A2), suggesting that D silver firs were more prone to drought-induced dieback  
497 due to their lower growth rate and production of smaller diameter tracheids (higher MND) as  
498 compared with ND trees (e.g., Camarero et al., 2017). A denser earlywood in the D trees is  
499 characterized by tracheids with narrow lumens and a decreased theoretical hydraulic  
500 conductivity which leads to low growth rates (Domec et al., 2009).

501

#### 502 *4.2. Changes in elements as early-warning signals of dieback*

503 Wood nutrient concentrations are element- and species specific (e.g., Hietz et al.,  
504 2015, Meerts, 2002, Penninckx et al. 2001), although decreasing cations concentrations from  
505 pith to outer heartwood (or to cambium) have been commonly observed in many different tree  
506 species. For example, this was the case of: Ca and Mn in *Fagus sylvatica* L. (Penninckx et al.  
507 2001); Ca in *Pinus uncinata* Ram. (Hevia et al., 2018), and other *Pinus* spp. (Peterson and  
508 Anderson, 1990), or Mn in *P.sylvestris* (Scharnweber et al., 2016)). Here, a declining trend

509 was also observed for Ca and Mn (Figs. 2, 3 and 4). The steady decline of cation stemwood  
510 contents from older to younger wood can be explained by the decreasing moisture content,  
511 non-structural carbohydrates concentrations and cation binding capacity with increasing  
512 distance from the pith to the bark (e.g., Bondietti et al., 1990; Momoshima and Bondietti,  
513 1990). Changes in concentration at the boundary between the heartwood and sapwood can be  
514 also sharp for some elements, as seen in our study for K (Fig. 3), in line with previous  
515 research (e.g., Hevia et al., 2018; Penninckx et al., 2001; Smith et al., 2014). Instead, our  
516 results for the concentration of most other elements did not change much between sapwood  
517 and heartwood in agreement with other species (e.g., Hevia et al., 2018; Hietz et al., 2015).  
518 Ultimately, the reduction of hydraulic conductivity and growth negatively affects the plant's  
519 nutrient status given the importance of active water flux along the soil-plant continuum for  
520 nutrient uptake (Salazar-Tortosa et al., 2018; Sardans et al., 2008, 2012). Moreover, the  
521 hydraulic properties of trees are modulated by changes in xylem sap cation concentrations  
522 (Nardini et al., 2011; Oddo et al., 2014), particularly K (see Fig. 3). Ca also plays a relevant  
523 role during cell division (White and Broadley, 2003) and the synthesis of cell walls (Eklund  
524 and Eliasson 1990), especially during latewood production (Lautner and Fromm, 2010;  
525 Sánchez-Salguero et al., 2019). Therefore, Ca availability may affect cambium dynamics and  
526 the rate of wood production and tracheid expansion (Fromm, 2010). Since Ca is an essential  
527 nutrient for tree metabolism and various physiological processes related to growth (e.g., St.  
528 Clair et al., 2005), hydraulic conductivity and tree vigor (Cronan and Grigal, 1995; Drohan et  
529 al., 2002; Houle et al., 2007 and others), low Ca concentrations are associated to growth  
530 decline (Bal et al., 2015). Along this, Mn is also essential for cell division and elongation  
531 (Seresinhe, 1996), and it is involved in many enzymatic activities and the structural  
532 stabilization of tissues (Guo et al., 2016).

533           When trees are subjected to drought stress, sapwood cation concentrations can  
534 increase to modulate hydraulic conductivity (Nardini et al., 2011). This is the case of K in  
535 silver fir wood (Oddo et al., 2014), with an increasing concentration in D trees as compared  
536 with ND trees after the 1980s (Fig. 3). This pattern matches with the increase in ED and the  
537 inferred decrease in tracheid lumen area and theoretical hydraulic conductivity (Pellizzari et  
538 al., 2016). An increase in xylem sap K content will compensate the loss of hydraulic  
539 conductivity (Trifilò et al., 2011), but prolonged drought stress can lead to K deficit and  
540 imbalance (Figs. 3 and 5) that might exacerbate hydraulic failure, and cause phloem  
541 dysfunction and carbon starvation (Salazar-Tortosa et al., 2018). Active upregulation of  
542 sapwood ion concentration under drought stress may enhance the hydraulic efficiency of  
543 viable xylem conduits, thus allowing plants to avoid catastrophic runaway embolism (Nardini  
544 et al., 2010). Plant Ca concentrations will also respond to drought (Bush, 1995), which  
545 reduces the uptake rates of this nutrient (Rouphael et al., 2012). Decreases in Ca  
546 concentrations can be also linked to a reduction in tracheid size due to a loss of turgor during  
547 xylogenesis (Pellizzari et al., 2016). This could explain the lower Ca concentrations we  
548 detected after 1980s droughts in the D silver fir trees (Fig. 3). In contrast, Mn can increase its  
549 accumulation in cells under water stress (Man et al., 2011), which would explain the higher  
550 Mn concentrations found in D trees up to five decades prior to the onset of the growth decline,  
551 suggesting that this element may serve as early-warning signals of impending dieback (see  
552 Figs. 2 and 4). In addition, under stress conditions plants deploy a strong P-mobilising  
553 strategy that increases the Mn concentrations of plant tissues (see Lambers et al., 2015),  
554 which explains the changes in Mn and P concentrations during the 1980s and 1990s droughts  
555 found in the D trees in both species (Fig. 4). These results are also consistent with dieback  
556 impacts on P uptake which may decrease as a consequence of the reduction in root activity  
557 (Avila et al., 2016; Schneider et al., 2001). Mn deficiency is a widespread problem, but more

558 pronounced in cool and wet environments (Alloway, 2008). High foliar Mn concentrations  
559 have been also related to low rates of photosynthesis (St. Clair et al., 2005) and impaired  
560 growth through metabolic interferences with other nutrient (El-Jaoual and Cox, 1998). The  
561 excess of Mn in the soil is toxic to many plants, and can inhibit the uptake of essential  
562 elements, such as Ca, K, Mg, Fe and P (Marschner, 2012; Millaleo et al., 2013). Mn  
563 interference with the uptake of other essential nutrients could explain the lower Mg:Mn, P:Mn  
564 or Ca:Mn ratios in wood of D trees for both species (Figs. 4, A3 and A4). High Mn  
565 concentrations in sapwood and leaves have also been considered as predisposing or  
566 contributing factors in forest dieback (e.g., Houle et al., 2007; Kogelman and Sharpe, 2006).  
567 Our findings agree with previous studies in which sugar maple (*Acer saccharum*) trees were  
568 predisposed to decline due to imbalances in Ca and Mn (cf. Hallett et al., 2006; Houle et al.,  
569 2007; Kogelmann and Sharpe, 2006). Divergent trends between D and ND trees were also  
570 found for Mg, Zn (annual) and Na (decadal) concentrations during the last decades, which  
571 agrees with previous studies on sugar maple in Canada (Côte and Camire, 1995; Houle et al.,  
572 2007). In particular, the sharp decline in wood Na concentration relative to ND trees further  
573 supports that D trees had lower hydraulic conductivity after the 1980s droughts in agreement  
574 with their reduction in tracheid size and growth rates.

575 All in all, divergence between vigor classes was more remarkable in the long-term for  
576 annual Mn, alone and combined with other elements in molar ratios (Ca:Mn, Mn:Al and  
577 P:Mn) (Figs. 2, 4 and A4). Several studies have recommended the use of molar ratios as better  
578 diagnostic of environmental changes (e.g., DeWalle et al., 1991; Hevia et al., 2018;  
579 Panyushkina et al., 2016); our results indicate that tree responses related to decline are  
580 stronger for Mn and its molar ratios, and can be traced back to several decades before the  
581 onset of the growth decline.

582

### 583 4.3. Associations between wood traits and changes in tree-ring nutrient concentrations

584 The concentration of elements in wood was strongly related to wood anatomy traits (see Table  
585 1 and Figs.6 and A6), given that secondary cell walls contain few ion exchange sites, which  
586 means that tissue with thick cell walls will have low concentrations of most elements (Hietz et  
587 al., 2015). In our study sites, xylem nutrient concentrations differed between D vs. ND trees,  
588 especially in the sapwood (Fig. 3). Our results confirmed that wood traits relationships with  
589 several key nutrients (e.g., Mn, P, Sr, K, Ca, Mg, Na) showed divergences between D and ND  
590 trees in both species (Figs. 3, 6 and A6). The models showed that Mn, Ca:Mn, Mg:Mn and  
591 P:Mn are strongly related to earlywood density (ED) in both species, conforming good  
592 indicators of long-term nutrient imbalances in relation to tracheid lumen size and hydraulic  
593 conductivity (Table A2; Figs. 6, A5 and A6). Our results showed also a strong relationship  
594 between Sr:Ca ratio and wood density as previously observed in other conifers (Silkin and  
595 Ekimova, 2012). The concentrations of these ions change with the development of different  
596 cell wall layers; Ca ion binding occurs more effectively in earlywood, whereas Sr is more  
597 effectively bound in latewood tracheids (Silkin and Ekimova, 2012) (Fig. A6). The behavior  
598 of Ca and Sr is almost identical for many forest biogeochemical processes (Drouet and  
599 Herbauts, 2008).

600 Improved nutrient status and plant N uptake could support the regrowth of tissue lost  
601 during drought (e.g., roots, foliage) resulting in improved resilience of trees to droughts  
602 (Gessler et al., 2017). Interestingly, N did not seem to be involved in these nutrient  
603 imbalances in D trees, since the high wood N:K and P:K ratios found in the D trees for the  
604 drought-sensitive silver fir, are largely indicative of strong K limitation of growth under low  
605 soil moisture conditions (Salazar-Tortosa et al., 2018; Urbina et al., 2015; see Fig. 5). The  
606 nutrient deficit and imbalance observed in D trees for both trees species could be related to  
607 20<sup>th</sup> century climate trends towards warmer and drier conditions (Urbina et al., 2015). The

608 N:P, N:K and P:K ratios were much higher at the xeric Scots pine site than at the mesic silver  
609 fir site (Fig. 5). This suggests that the severe nutrient imbalance in Scots pine was largely the  
610 result of chronic drought-induced stress, rather than of low soil nutrient availability (Salazar-  
611 Tortosa et al., 2018). This stoichiometric imbalance can impair photosynthesis, transpiration,  
612 water-use efficiency and growth (Sardans and Peñuelas, 2012, 2015). Moreover, our results  
613 highlight the need to further explore nutrient dynamics in the drought-induced tree mortality  
614 framework, particularly under forecasted hotter droughts (Gessler et al., 2017).

615

#### 616 *4.4. Soil chemical properties and differences between tree vigor classes*

617 Soil drying can also alter nutrient availability to trees (Sardans and Peñuelas, 2007), in  
618 addition to the observed site differences in nutrients (Table A5). Although soil nutrient  
619 availability is highly heterogeneous at multiple spatial and temporal scales (Ettema and  
620 Wardle, 2002), our results showed a strong variation between the two vigor classes (Table  
621 A5), with higher values of several elements below D trees. This could be explained if D trees  
622 are located in particularly dry microsites (e.g., Lloret et al., 2015; Matías et al., 2011) where  
623 root and microbial activity are partially constrained by low soil moisture (Bal et al., 2015).  
624 Soil physical and chemical properties such as low water-holding capacity largely affected by  
625 soil hydrophobicity (water repellence), and nutrient deficiency can exacerbate the negative  
626 consequences of drought stress on tree vigour leading to forest die-off (Pinto and Peñuelas,  
627 2007; Gazol et al., 2018). This makes therefore difficult to know if differences in soil  
628 nutrients could also explain the forest dieback or they arise as a consequence of this process  
629 (Gazol et al., 2018). On one hand, soil nutrients like Ca, Mg, K, and Na are mainly cycled  
630 through mineral weathering (Gallardo, 2003), but also by biological pumping through leaf  
631 litter decomposition (Lucas, 2001). For this reason, an increased needle shedding of D trees  
632 could be associated to an increased nutrient input if fine-root and mycorrhiza activity has not

633 diminished. On the other hand, the higher nutrient concentration in soils for D trees could  
634 predispose to dieback due to maladaptive drought survival in relation to tree nutrient uptake  
635 (Gessler et al., 2017). In addition, the uptake of nutrients with limited mobility and diffusion  
636 rates in soil (for example, P, Zn, Cu) may be particularly vulnerable to severe decreases in  
637 transpiration and mass flow to roots during consecutive droughts, compared to mobile  
638 nutrients as N (Rengel and Marschner, 2005; Salazar-Tortosa et al., 2018).

639

#### 640 *4.5. Dendrochemistry improves the understanding of drought-induced forest dieback*

641 Soil chemistry data and leaf nutrient measurements have been considered good predictors of  
642 tree vulnerability to forest decline (Bailey et al., 2004; Vitousek, 2004). Our novel tree-ring  
643 nutrients approach provides a more dynamic assessment of nutritional conditions across  
644 multiple growing seasons (e.g., Hevia et al., 2018; Sánchez-Salguero et al., 2019). Future  
645 research should investigate if the relationships between long-term wood traits, genetic  
646 predisposition and soil features can determine the contrasting susceptibility of neighboring  
647 trees to dieback, since tree-rings can reflect the behavior of individual trees and underlying  
648 soil during the year of ring formation but also capture historical legacy effects (Bondietti and  
649 McLaughlin, 1992).

650 As expected, pooling chemical data (ICP-OES) showed significant relationships with  
651 averaged decadal values by  $\mu$ XRF (Fig. A1), but revealed differences in the long-term trends  
652 and did not capture clear divergences (Figs. 2 and 4; Table A5). In this sense, pooling wood  
653 material from decadal blocks of several trees excludes the statistical uncertainty associated  
654 with inter-tree variability (c.f. Dorado-Liñán et al., 2011).

655

## 656 **5. Conclusions**

657 We found that D trees presented lower radial growth rates and higher earlywood wood density  
658 than ND trees, but these differences were more pronounced and started before in silver fir  
659 than in Scots pine. Silver fir and Scots pine D trees showed Mn and Ca imbalances (along  
660 with K starvation and imbalance in Scots pine), and such alterations in wood nutrient  
661 concentrations are coherent with hydraulic failure due to severe drought stress. We propose  
662 the use of Mn and related ratios (Ca:Mn, Mn:Al or P:Mn) as early-warning signals of forest  
663 dieback since they diverged between D and ND trees several decades before the growth  
664 decline onset. This divergence was very clear in Silver fir, a species with a good potential for  
665 dendrochemistry studies related to dieback. This study highlights the potential of  $\mu$ XRF  
666 methods to reveal long-term macro- and micro-nutrients changes and imbalances in trees at  
667 seasonal to annual scales.

668

#### 669 **Acknowledgements**

670 This study was supported by projects FunDiver (CGL2015-69186-C2-1-R), CoMo-ReAdapt  
671 (CGL2013-48843-C2-1-R), AMB95-0160, CGL2011-26654 (Spanish Ministry of Economy,  
672 Industry and Competitiveness) and EU projects: CANOPEE (Interreg V-A POCTEFA 2014-  
673 2020-FEDER funds). The authors are grateful to Juan Majada for providing support for this  
674 study, Laura González Sánchez and Elena Lahoz who assisted in the laboratory. RSS and  
675 GSB were supported by a Postdoctoral grant (IJCI-2015-25845 and FJCI 2016-30121,  
676 respectively, FEDER funds). We thank the editor E. Paoletti and two anonymous reviewers  
677 for improving the manuscript.

678

679 The authors declare no conflict of interest.

680

681

682

- 684 Adams H.D., Zeppel M.J.B., Anderegg W.R.L., Hartmann H., Landhäusser S.M., Tissue D.T., Huxman T.E.,  
685 Hudson P.J., Franz T.E., Allen C.D., Anderegg L.D.L., Barron-Gafford G.A., Beerling D.J., Breshears  
686 D.D., Brodribb T.J., Bugmann H., Cobb R.C., Collins A.D., Dickman L.T., Duan H., Ewers B.E.,  
687 Galiano L., Galvez D.A., Garcia-Forner N., Gaylord M.L., Germino M.J., Gessler A., Hacke U.G.,  
688 Hakamada R., Hector A., Jenkins M.W., Kane J.M., Kolb T.E., Law D.J., Lewis J.D., Limousin J.M.,  
689 Love D.M., Macalady A.K., Martínez-Vilalta J., Mencuccini M., Mitchell P.J., Muss J.D., O'Brien M.J.,  
690 O'Grady A.P., Pangle R.E., Pinkard E.A., Piper F.I., Plaut J.A., Pockman W.T., Quirk J., Reinhardt K.,  
691 Ripullone F., Ryan M.G., Sala A., Sevanto S., Sperry J.S., Vargas R., Venetier M., Way D.A., Xu C.,  
692 Yezpe E.A., McDowell N.G. (2017). A multi-species synthesis of physiological mechanisms in  
693 drought-induced tree mortality. *Nature Ecology and Evolution*, 1, 1285-1291.
- 694 Allen C.D., Macalady A.K., Chenchouni H., Bachelet D., McDowell N., Venetier M., Kitzberger T, Rigling A.,  
695 Breshears, D.D., Hogg E.H. (Ted), González P., Fensham R., Zhang Z., Castro J., Demidova N., Lim H-  
696 H., Allard G., Running S.W., Semerci A., Cobb N. (2010). A global overview of drought and heat-  
697 induced tree mortality reveals emerging climate change risks for forests. *Forest Ecology and*  
698 *Management*, 259, 660-684.
- 699 Alloway B.J. (2008). *Micronutrient Deficiencies in Global Crop Production*. Dordrecht, The Netherlands:  
700 Springer.
- 701 Anderegg W.R.L., Schwalm C., Biondi F., Camarero J.J., Koch G., Litvak M., Ogle K., Shaw J.D., Shevliakova  
702 E., Williams A.P., Wolf A., Ziaco E., Pacala S. (2015). Pervasive drought legacies in forest ecosystems  
703 and their implications for carbon cycle models. *Science*, 349(6247), 528-532.
- 704 Avila J.M., Gallardo A., Ibáñez B., Gómez-Aparicio L. (2016). *Quercus suber* dieback alters soil respiration and  
705 nutrient availability in Mediterranean forests. *Journal of Ecology*, 104, 1441-1452.
- 706 Bailey S.W., Horsley S.B., Long, R.P., Hallett R.A. (2004). Influence of edaphic factors on sugar maple  
707 nutrition and health on the Alleghany Plateau. *Soil Science Society of America Journal*, 68, 243-252.
- 708 Bal T.L., Storer A.J., Jurgensen M.F., Doskey P.V., Amacher M.C. (2015). Nutrient stress predisposes and  
709 contributes to sugar maple dieback across its northern range: a review. *Forestry*, 88(1), 64-83.
- 710 Balouet J.C., Chalot M. (2015). *Pollution Investigations by Trees. Methodological guide*, Ademe, France.
- 711 Barton K. (2012). MuMIn: multi-model inference. R package version 1.0.0. Available at: [http://CRAN.R-](http://CRAN.R-project.org/package=MuMIn)  
712 [project.org/package=MuMIn](http://CRAN.R-project.org/package=MuMIn).
- 713 Bondietti E.A., McLaughlin S.B. (1992). Evidence of historical influences of acidic deposition on wood and soil  
714 chemistry. In: D.W. Johnson and S.E. Lindberg (Eds.), *Ecological Studies 91: Atmospheric Deposition*  
715 *and Forest Nutrient Cycling* (pp. 358-377). New York: SpringerVerlag.
- 716 Bondietti E.A., Momoshima N., Shortle W.C., Smith K.T. (1990) A historical perspective on divalent cation  
717 trends in red spruce stemwood and the hypothetical relationship to acidic deposition. *Canadian Journal*  
718 *of Forest Research*, 20, 1850-1858.
- 719 Bréda N., Huc R., Granier A., Dreyer E. (2006). Temperate forest trees and stands under severe drought: a review  
720 of ecophysiological responses, adaptation processes and long-term consequences. *Annals of Forest*  
721 *Science*, 63, 625-644.
- 722 Bunn A., Korpela M., Biondi F., Campelo F., Mérian P., Qeadan F., Zang C, Pucha-Cofrep D., Wernicke J.  
723 (2018). dplR: Dendrochronology Program Library in R. R package version 1.6.9.
- 724 Burnham K.P., Anderson D.R. (2002). *Model Selection and Multimodel Inference: a Practical Information-*  
725 *theoretic Approach*. New York: Springer.
- 726 Bush D.S. (1995). Calcium Regulation in Plant Cells and its Role in Signaling *Annual Review of Plant*  
727 *Physiology and Plant Molecular Biology*, 46, 95-122.
- 728 Cailleret M., Jansen S., Robert E.M., Desoto L., Aakala T., Antos J.A., Beikircher B., Bigler C., Bugmann H.,  
729 Caccianiga M., Čada V., Camarero J.J., Cherubini P., Cochard H., Coyea M.R., Čufar K., Das A.J.,  
730 Davi H., Delzon S., Dorman M., Gea-Izquierdo G., Gillner S., Haavik L.J., Hartmann H., Hereş A.M.,  
731 Hultine K.R., Janda P., Kane J.M., Kharuk V.I., Kitzberger T., Klein T., Kramer K., Lens F., Levanic  
732 T., Linares J.C., Lloret F., Lobo-Do-Vale R., Lombardi F., López Rodríguez R., Mäkinen H., Mayr S.,  
733 Mészáros I., Metsaranta J.M., Minunno F., Oberhuber W., Papadopoulos A., Peltoniemi M., Petritan  
734 A.M., Rohner B., Sangüesa-Barreda G. Sarris D., Smith J.M., Stan A.B., Sterck F., Stojanović D.B.,  
735 Suarez M.L., Svoboda M., Tognetti R., Torres-Ruiz J.M., Trotsiuk V., Villalba R., Vodde F., Westwood  
736 A.R., Wyckoff P.H., Zafirov N., Martínez-Vilalta J. (2017). A synthesis of radial growth patterns  
737 preceding tree mortality. *Global Change Biology*, 23, 1675-1690.
- 738 Camarero J.J., Bigler C., Linares J.C., Gil-Pelegrin E. (2011). Synergistic effects of past historical logging and  
739 drought on the decline of Pyrenean silver fir forests. *Forest Ecology and Management*, 262, 759-769.

740 Camarero J.J., Fernández-Pérez L., Kirilyanov A.V., Shestakova T.A., Knorre A.A., Kukarskih V.V., Voltas J.  
741 (2017). Minimum wood density of conifers portrays changes in early season precipitation at dry and  
742 cold Eurasian regions. *Trees*, 31(5), 1423-1437.

743 Camarero J.J., Gazol A., Sangüesa-Barreda G., Cantero-Fariña A., Sánchez-Salguero R., Sanchez-Miranda A.,  
744 Granda E., Serra-Maluquer X., Ibañez R. (2018). Forest growth responses to drought at short- and long-  
745 term scales in Spain: squeezing the stress memory from tree rings. *Frontiers in Ecology and Evolution*,  
746 6(9), 1-11.

747 Camarero J.J., Gazol A., Sangüesa-Barreda G., Oliva J., Vicente-Serrano S.M. (2015). To die or not to die: early  
748 warnings of tree dieback in response to a severe drought. *Journal of Ecology*, 103, 44-57.

749 Carrer M., Unterholzner L., Castagneri D. (2018). Wood anatomical traits highlight complex temperature  
750 influence on *Pinus cembra* at high elevation in the Eastern Alps. *International Journal of*  
751 *Biometeorology*, 62(9), 1745-1753.

752 Côté B., Camire, C. (1995). Application of leaf, soil, and tree-ring chemistry to determine the nutritional status of  
753 sugar maple on sites of different levels of decline. *Water, Air, and Soil Pollution*, 83(3-4), 363-373.

754 Colangelo M., Camarero J.J., Battipaglia G., Borghetti M., De Micco V., Gentilesca T., Ripullone F. (2017). A  
755 multi-proxy assessment of dieback causes in a Mediterranean oak species. *Tree Physiology*, 37(5), 617-  
756 631.

757 Cronan C.S., Grigal, D.F. (1995). Use of calcium/aluminum ratios as indicators of stress in forest ecosystems.  
758 *Journal of Environmental Quality*, 24, 209-226.

759 Croudace I.W., Rindby A., Rothwel, R.G. (2006). ITRAX: description and evaluation of a new multi-function  
760 X-ray core scanner. In: R.G. Rothwell (Ed.), *New Techniques in Sediment Core Analysis* (pp. 51-63).  
761 London: Geological Society.

762 Dalla-Salda G., Martinez-Meier A., Cochard H., Rozenberg P. (2009). Variation of wood density and hydraulic  
763 properties of Douglas-fir (*Pseudotsuga menziesii* (Mirb.) Franco) clones related to a heat and drought  
764 wave in France. *Forest Ecology and Management*, 257(1), 182-189.

765 DeWalle D.R., Swistock B.R., Sayre R.G., Sharpe W.E. (1991). Spatial variations of sapwood chemistry with  
766 soil acidity in Appalachian forests. *Journal of Environmental Quality*, 20, 486-491.

767 Dobbertin M. (2005). Tree growth as indicator of tree vitality and of tree reaction to environmental stress: a  
768 review. *European Journal of Forest Research*, 124, 319-333.

769 Domec J.C., Warren J.M., Meinzer F.C., Lachenbruch B. (2009). Safety factors for xylem failure by implosion  
770 and air-seeding within roots, trunks and branches of young and old conifer trees. *IAWA Journal*, 30(2),  
771 101-120.

772 Dorado-Liñán I., Gutiérrez E., Helle G., Heinrich I., Andreu-Hayles L., Planells O., Leuenberger M., Bürger C.,  
773 Schleser G. (2011). Pooled versus separate measurements of tree-ring stable isotopes. *Science of the*  
774 *Total Environment*, 409(11), 2244-2251

775 Drohan P.J., Stout S.L., Petersen G.W. (2002). Sugar maple (*Acer saccharum* Marsh.) decline during 1979-1989  
776 in northern Pennsylvania. *Forest Ecology and Management*, 170, 1-17.

777 Drouet Th., Herbauts J. (2008). Evaluation of the mobility and discrimination of Ca, Sr and Ba in forest  
778 ecosystems: consequence on the use of alkaline-earth element ratios as tracers of Ca. *Plant and Soil*,  
779 302, 105-124.

780 Duchesne L., Ouimet R., Houle D. (2002). Basal area growth of sugar maple in relation to acid deposition, stand  
781 health, and soil nutrients. *Journal of Environmental Quality*, 31, 1676-1683.

782 Eklund L., Eliasson L. (1990). Effects of calcium ion concentration on cell wall synthesis. *Journal of*  
783 *Experimental Botany*, 41, 863-867.

784 El-Jaoual T., Cox D.A. (1998). Manganese toxicity in plants. *Journal of Plant Nutrition*, 21, 353-386.

785 Ettema C.H., Wardle D.A. (2002). Spatial soil ecology. *Trends in Ecology and Evolution*, 17, 177-183.

786 Fritts H.C. (2001). *Tree Rings and Climate*. Caldwell: Blackburn Press.

787 Fromm J. (2010). Wood formation of trees in relation to potassium and calcium nutrition. Invited Review: Part  
788 of an invited issue on tree nutrition. *Tree Physiology*, 30, 1140-1147.

789 Gallardo A. (2003). Spatial variability of soil properties in a floodplain forest in Northwest Spain. *Ecosystems*,  
790 6, 564-576.

791 Galván J.D., Camarero J.J., Gutiérrez E. (2014). Seeing the trees for the forest: drivers of individual growth  
792 responses to climate in *Pinus uncinata* mountain forests. *Journal of Ecology*, 102, 1244-1257.

793 Galván J.D., Camarero J.J., Sangüesa-Barreda G., Alla A.Q., Gutiérrez E. (2012). Sapwood area drives growth  
794 in mountain conifer forests. *Journal of Ecology*, 100(5), 1233-1244.

795 Gazol A., Camarero J.J. (2016). Functional diversity enhances silver fir growth resilience to an extreme drought.  
796 *Journal of Ecology*, 104, 1063-1075.

797 Gazol A., Camarero J.J., Jiménez J.J., Moret-Fernández D., López M.V., Sangüesa-Barreda G., Igual J.M.  
798 (2018). Beneath the canopy: Linking drought-induced forest die off and changes in soil properties.  
799 *Forest Ecology and Management*, 422, 294-302.

800 Gessler A., Keitel C., Nahm M., Rennenberg H. (2004). Water shortage affects the water and nitrogen balance in  
801 central European beech forests. *Plant Biology*, 6, 289-298.

802 Gessler A., Schaub M., McDowell N.G. (2017). The role of nutrients in drought-induced tree mortality and  
803 recovery. *New Phytologist*, 214, 513-520.

804 Guo W., Nazim H., Liang Z., Yang D. (2016). Magnesium deficiency in plants: An urgent problem. *The Crop*  
805 *Journal*, 4(2), 83-91.

806 Hallett R.A., Bailey, S.W., Horsley, S.B., Long, R.P. (2006). Influence of nutrition and stress on sugar maple at  
807 a regional scale. *Canadian Journal of Forest Research*, 36, 2235-2246.

808 Helama S., Läänelaid A., Raisio J., Tuomenvirta H. (2009). Oak decline in Helsinki portrayed by tree-rings,  
809 climate and soil data. *Plant Soil*, 319, 163-174.

810 Hevia A., Sánchez-Salguero R., Camarero J.J., Buras A., Sangüesa-Barreda G., Galván J.D., Gutiérrez E. (2018).  
811 Towards a better understanding of long-term wood-chemistry variations in old-growth forests: A case  
812 study on ancient *Pinus uncinata* trees from the Pyrenees. *Science of the Total Environment*, 625, 220-  
813 232.

814 Hietz P., Horsky M., Prohaska T., Lang I., Grabner M. (2015). High-resolution densitometry and elemental  
815 analysis of tropical wood. *Trees*, 29, 487-497.

816 Holmes R.L. (1983). Computer-assisted quality control in tree-ring dating and measurement. *Tree-ring Bulletin*,  
817 43, 69-78.

818 Horsley S.B., Long R.P., Bailey S.W., Hallett R.A., Hall T.J. (2000). Factors associated with the decline disease  
819 of sugar maple on the Allegheny Plateau. *Canadian Journal of Forest Research*, 30, 1365-1378.

820 Houle D., Tremblay S., Ouimet R. (2007). Foliar and wood chemistry of sugar maple along a gradient of soil  
821 acidity and stand health. *Plant and Soil*, 300(1-2), 173-183.

822 Hsiao T. (1973). Plant responses to water stress. *Annual review of Plant Physiology*, 24, 519-570.

823 Irvine J., Perks M.P., Magnani F., Grace J. (1998). The response of *Pinus sylvestris* to drought: stomatal control  
824 of transpiration and hydraulic conductance. *Tree Physiology*, 18, 393-402.

825 Kogelmann W.J., Sharpe W.E. (2006). Soil acidity and manganese in declining and nondeclining sugar maple  
826 stands in Pennsylvania. *Journal of Environmental Quality*, 35, 433-441.

827 Kuang Y.W., Wen D.Z., Zhou G.Y., Chu G.W., Sun F.F., Li J. (2008). Reconstruction of soil pH by  
828 dendrochemistry of Masson pine at two forested sites in the Pearl River Delta, South China. *Annals of*  
829 *Forest Science*, 65(8), 804.

830 Lachenbruch B., McCulloh K. (2014). Traits, properties, and performance: how woody plants combine hydraulic  
831 and mechanical functions in a cell, tissue, or whole plant. *New Phytologist*, 204, 747-764.

832 Lambers H., Hayes P.E., Laliberte E., Oliveira R.S., Turner B.L. (2015). Leaf manganese accumulation and  
833 phosphorus-acquisition efficiency. *Trends in Plant Science*, 20, 83-90.

834 Lautner S., Fromm J. (2010). Calcium-dependent physiological processes in trees. *Plant Biology*, 12, 268-274.

835 Levanic T., Cater M., McDowell N.G. (2011). Associations between growth, wood anatomy, carbon isotope  
836 discrimination and mortality in a *Quercus robur* forest. *Tree Physiology*, 31(3), 298-308.

837 Lloret F., Mattana S., Curiel Yuste, J. (2015). Climate-induced die-off affects plant-soil-microbe ecological  
838 relationship and functioning. *FEMS Microbiology Ecology*, 91, 1-12.

839 Lucas Y. (2001). The role of plants in controlling rates and products of weathering: importance of biological  
840 pumping. *Annual Review of Earth and Planetary Sciences*, 29, 135-163.

841 Man D., Yong-Xia Bao Y.X., Han L.B., Zhang X. (2011). Drought tolerance associated with proline and  
842 hormone metabolism in two tall fescue cultivars. *HortScience*, 46, 1027-1032.

843 Manion P.D. (1991). *Tree disease concepts*. Englewood Cliffs, N.J.: Prentice-Hall.

844 Marschner P. (2012). *Marschner's Mineral Nutrition of Higher Plants*. Boston, M.A.: Academic Press.

845 Matías L., Castro J., Zamora R. (2011). Soil-nutrient availability under a global-change scenario in a  
846 Mediterranean mountain ecosystem. *Global Change Biology*, 14(4), 1646-1657.

847 McDowell N., Pockman W.T., Allen C.D., Breshears D.D., Cobb N., Kolb T., Plaut J., Sperry J., West A.,  
848 Williams D.G., Yepez E.A. (2008). Mechanisms of plant survival and mortality during drought: why do  
849 some plants survive while others succumb to drought? *New phytologist*, 178(4), 719-739.

850 Millaleo R., Reyes-Díaz M., Alberdi M., Ivanov A.G., Krol M., Huner N.P. (2013). Excess manganese  
851 differentially inhibits photosystem I versus II in *Arabidopsis thaliana*. *Journal of Experimental Botany*,  
852 64, 343-353.

853 Momoshima N., Bondietti E.A. (1990). Cation binding in wood: applications to understanding historical changes  
854 in divalent cation availability to red spruce. *Canadian Journal of Forest Research*, 20(12): 1840-1849.

855 Muller B., Pantin F., Génard M., Turc O., Freixes S., Piques M., Gibon Y. (2011). Water deficits uncouple  
856 growth from photosynthesis, increase C content, and modify the relationship between C and growth in  
857 sink organs. *Journal of Experimental Botany*, 62(6), 1715-1729.

858 Nakagawa S, Schielzeth H. (2013). A general and simple method for obtaining  $R^2$  from generalized linear  
859 mixed-effects models. *Methods in Ecology and Evolution*, 4, 133-142.

860 Nardini A., Grego F., Triflò P., Salleo S. (2010). Changes of xylem sap ionic content and stem hydraulics in  
861 response to irradiance in *Laurus nobilis*. *Tree Physiology*, 30, 628-635.

862 Nardini A., Salleo S., Jansen S. (2011). More than just a vulnerable pipeline: xylem physiology in the light of  
863 ion-mediated regulation of plant water transport. *Journal of Experimental Botany*, 62, 4701-4718.

864 Oddo, E., Inzerillo, S., Grisafi, F., Sajeve, M., Salleo, S. Nardini, A. (2014). Does short-term potassium  
865 fertilization improve recovery from drought stress in laurel? *Tree Physiology* 34, 906-913.

866 Panyushkina I.P., Shishov V.V., Grachev A.M., Knorre A.A., Kirdeyanov A.V., Leavitt S.W., Vaganov E.A.,  
867 Chebykin E.P., Zhuchenko N.A., Hughes M.K. (2016). Trends in elemental concentrations of tree rings  
868 from the Siberian Arctic. *Tree Ring Research*, 72, 67-77.

869 Pellizzari E., Camarero J.J., Gazol A., Sangüesa-Barreda G., Carrer M. (2016). Wood anatomy and carbon-  
870 isotope discriminations support long-term hydraulic deterioration as a major cause of drought-induced  
871 dieback. *Global Change Biology*, 22, 2125-2137.

872 Penninckx V., Glineur, S., Gruber, W., Herbauts, J., Meerts, P. (2001). Radial variations in wood mineral  
873 element concentrations: a comparison of beech and pedunculate oak from the Belgian Ardennes. *Annals*  
874 *of Forest Science*, 58, 253-260.

875 Pinheiro J.C., Bates D.M. (2000). *Mixed-Effects Models in S and S-PLUS*, New York, NY, USA: Springer.

876 Pinheiro J., Bates D., DebRoy S., Sarkar D. R Core Team (2014). *nlme: Linear and Nonlinear Mixed Effects*  
877 *Models*. R package version 3.1-117.

878 Pinto, J., Peñuelas, J. (2007) Drought changes phosphorus and potassium accumulation patterns in an evergreen  
879 Mediterranean forest. *Functional Ecology* 21, 191-201.

880 R Development Core Team (2019). *R: A Language and Environment for Statistical Computing*, R Foundation  
881 for Statistical Computing, Vienna, Austria. Available at: <http://www.R-project.org>.

882 Rengel Z., Marschner P. (2005). Nutrient availability and management in the rhizosphere: Exploiting genotypic  
883 differences. *New Phytologist*, 168, 305-312.

884 Rouphael Y, Cardarelli M, Schwarz D, Franken P, Colla G. (2012). Effects of drought on nutrient uptake and  
885 assimilation in vegetable crops. In: R. Aroca (Ed.), *Plant responses to drought stress* (pp. 171-195).  
886 Berlin, Heidelberg, Germany: Springer.

887 Rozas V., Sampedro L. (2013). Soil chemical properties and dieback of *Quercus robur* in Atlantic wet forests  
888 after a weather extreme. *Plant and Soil*, 373, 673-685.

889 Salazar-Tortosa D., Castro J., Villar-Salvador P., Viñebla B., Matías L., Michelsen A., Rubio de Casas R.,  
890 Querejeta J.I. (2018). The “isohydric trap”: A proposed feedback between water shortage, stomatal  
891 regulation, and nutrient acquisition drives differential growth and survival of European pines under  
892 climatic dryness. *Global Change Biology*, 24(9), 4069-4083

893 Sánchez-Salguero R., Camarero J.J., Gutiérrez E., González Rouco F., Gazol A., Sangüesa-Barreda G., Andreu-  
894 Hayles L., Linares J.C., Seftigen K. (2017). Assessing forest vulnerability to climate warming using a  
895 process-based model of tree growth: bad prospects for rear-edges. *Global Change Biology*, 23(7), 2705-  
896 2719.

897 Sánchez-Salguero R., Camarero J.J., Hevia A., Sangüesa-Barreda G., Galván J.D., Gutiérrez E. (2019). Testing  
898 annual tree-ring chemistry by X-ray fluorescence for dendroclimatic studies in high-elevation forests  
899 from the Spanish Pyrenees. *Quaternary International*, 514, 130-140.

900 Sangüesa-Barreda G., Linares J.C., Camarero J.J. (2015). Reduced growth sensitivity to climate in bark-beetle  
901 infested Aleppo pines: Connecting climatic and biotic drivers of forest dieback. *Forest Ecology and*  
902 *Management*, 357, 126-137.

903 Sardans J., Peñuelas J. (2007). Drought changes phosphorus and potassium accumulation patterns in an  
904 evergreen Mediterranean forest. *Functional Ecology*, 21, 191-201.

905 Sardans J., Peñuelas J. (2012). The role of plants in the effects of global change on nutrient availability and  
906 stoichiometry in the plant-soil system. *Plant Physiology*, 160, 1741-1761.

907 Sardans J., Peñuelas J. (2015). Potassium: A neglected nutrient in global change. *Global Ecology and*  
908 *Biogeography*, 24, 261-275.

909 Sardans, J., Peñuelas, J., Coll, M., Vayreda, J., Rivas-Ubach, A. (2012). Stoichiometry of potassium is largely  
910 determined by water availability and growth in Catalanian forests. *Functional Ecology*, 26, 1077-1089.

911 Sardans J., Peñuelas J., Prieto P., Stiarte M. (2008). Changes in Ca, Fe, Mg, Mo, Na and S content in a  
912 Mediterranean shrubland under warming and drought. *Journal of Geophysical research*, 113, G03039.

913 Scharnweber T., Hevia A., Buras A., van der Maaten E., Wilmking M. (2016). Common trends in elements?  
914 Within- and between-tree variations of wood-chemistry measured by X-ray fluorescence - A  
915 dendrochemical study. *Science of the Total Environment*, 566-567, 1245-1253.

916 Schlesinger W.H., Dietze M.C., Jackson R.B., Phillips R.P., Rhoades C.C., Rustad L.E., Vose J.M. (2016).  
917 Forest biogeochemistry in response to drought. *Global Change Biology*, 22, 2318-2328.

918 Schneider K., Turrión M.B., Grierson P.F., Gallardo, J.F. (2001). Phosphatase activity, microbial phosphorus,  
919 and fine root growth in forest soils in the Sierra de Gata, western central Spain. *Biology and Fertility of*  
920 *Soils*, 34, 151-155.

921 Schweingruber F.H. (1996). *Tree Rings and Environment Dendroecology*. Bern: Paul Haupt.

922 Seresinhe P.S.J.W. (1996). The effect of manganese on the growth of tomato cells in suspension culture. *Journal*  
923 *of the National Science Foundation of Sri Lanka*, 24, 267-278.

924 Sevanto S., McDowell N.G., Dickman L.T., Pangle R., Pockman W.T. (2014). How do trees die? A test of the  
925 hydraulic failure and carbon starvation hypotheses. *Plant, Cell and Environment*, 37, 153-161.

926 Silkin P.P., Ekimova N.V. (2012). Relationship of strontium and calcium concentrations with the parameters of  
927 cell structure in Siberian spruce and fir tree-rings. *Dendrochronologia*, 30, 189-194.

928 Smith K.T., Balouet J.C., Sortle W.C., Chalot M., Beaujard F., Grudd H., Vroblecky D.A., Burken J.G. (2014).  
929 Dendrochemical patterns of calcium, zinc and potassium related to internal factors detected by energy  
930 dispersive X-ray fluorescence (EDXRF). *Chemosphere*, 95, 58-62.

931 St. Clair S.B., Carlson J.E., Lynch J.P. (2005). Evidence for oxidative stress in sugar maple stands growing on  
932 acidic nutrient imbalanced forest soils. *Oecologia*, 145, 258-269.

933 St. Clair S.B., Sharpe W.E., Lynch J.P. (2008). Key interactions between nutrient limitation and climatic factors  
934 in temperate forests: a synthesis of the sugar maple literature. *Canadian Journal of Forest Research*, 38,  
935 401-414.

936 Szczepkowski A., Nicewicz D. (2008). The content of heavy metals in the wood of healthy and dying oak trees  
937 (*Quercus robur L.*, *Q. petraea* (Matt.) Liebl.). *Acta Scientiarum Polonorum Silvarum Colendarum Ratio*  
938 *et Industria Lignaria*, 7, 55-65.

939 Timofeeva G., Treydte K., Bugmann H., Rigling A., Schaub M., Siegwolf R., Saurer M. (2017). Long-term  
940 effects of drought on tree-ring growth and carbon isotope variability in Scots pine in a dry environment.  
941 *Tree Physiology*, 37, 1028-1041.

942 Trifilò P., Nardini A., Raimondo F., Lo Gullo M.A., Salleo S. (2011). Ion-mediated compensation for drought-  
943 induced loss of xylem hydraulic conductivity in field-growing plants of *Laurus nobilis*. *Functional Plant*  
944 *Biology*, 38, 606-613.

945 Urbina I., Sardans J., Beierkuhnlein C., Jentsch A., Backhaus S., Grant K., Kreyling J., Peñuelas J. (2015). Shifts  
946 in the elemental composition of plants during a very severe drought. *Environmental and Experimental*  
947 *Botany*, 111, 63-73.

948 Vitousek P.M. (2004). *Nutrient Cycling and Limitation: Hawai'i as a Model System*. Princeton Environmental  
949 *Institute Series*.

950 Voltas J., Camarero J.J., Carulla D., Aguilera M., Ortiz A., Ferrio J.P. (2013). A retrospective, dual-isotope  
951 approach reveals individual predispositions to winter-drought induced tree dieback in the southernmost  
952 distribution limit of Scots pine. *Plant, Cell and Environment*, 36, 1435-1448.

953 White P.J., Broadley M.R. (2003). Calcium in plants. *Annals of Botany*, 92(4), 487-511.

954 William R.W., Cleveland C., Kolby Smith W., Todd-Brown K. (2015). Future productivity and carbon storage  
955 limited by terrestrial nutrient availability. *Nature Geoscience*, 8, 441-444.

956 Wood S.N. (2006). *Generalized Additive Models: An Introduction with R*. Boca Raton: Chapman and Hall, CRC  
957 *Press*.

958 Yoshimura K., Saiki S.T., Yazaki K., Ogasa M.Y., Shirai M., Nakano T., Yoshimura J., Ishida A. (2016). The  
959 dynamics of carbon stored in xylem sapwood to drought-induced hydraulic stress in mature trees.  
960 *Scientific reports – Nature*, 6, 24513.

961